HHS Public Access

Author manuscript

ACS Biomater Sci Eng. Author manuscript; available in PMC 2024 May 08.

Published in final edited form as:

ACS Biomater Sci Eng. 2023 May 08; 9(5): 2103–2128. doi:10.1021/acsbiomaterials.1c01208.

Bioinspired Materials for Wearable Devices and Point-of-Care Testing of cancer

Raj Shankar Hazra[1], **Md Rakib Hasan Khan**[2], **Narendra Kale**[3], **Tabassum Tanha**[4], **Jayant Khandare**[3,5,6], **Sabha Ganai**[7,8], **Mohiuddin Quadir**[1,2,9,*]

[1]Materials and Nanotechnology Program, North Dakota State University, Fargo, ND 58108, United States

[2]Biomedical Engineering Program, North Dakota State University, Fargo, ND 58108, United States

[3]Actorius Innovations and Research Pvt. Ltd., Pune, 411057 India

[4]Genomics and Bioinformatics Program, North Dakota State University, Fargo, ND 58108, United States

[5]School of Pharmacy, Dr. Vishwananth Karad MIT World Peace University, Kothrud, Pune 411038, India.

[6]School of Consciousness, MIT WPU, Kothrud, Pune 411038, India.

[7]Division of Surgical Oncology, Sanford Research, Fargo, North Dakota 58122, United States

[8]Complex General Surgical Oncology, University of North Dakota, Grand Forks, ND 58202, United States

[9]Department of Coatings and Polymeric Materials, North Dakota State University, Fargo, ND 58108, United States

Abstract

Wearable, point-of-care diagnostics, and biosensors are on the verge of bringing transformative changes in detection, management, and treatment of cancer. Bio-inspired materials with new forms and functions have frequently been used, in both translational and commercial spaces, to fabricate such diagnostic platforms. Engineered from organic or inorganic molecules, bio-inspired systems are naturally equipped with biorecognition and stimuli-sensitive properties. Mechanism of action of bio-inspired materials are deeply connected with thermodynamically or kinetically controlled self-assembly at molecular and supramolecular level. Thus, integration of bio-inspired materials into wearable devices, either as triggers or sensors, brings about unique device properties usable for detection, capture, or rapid read-out for an analyte of interest. In this review, we present the basic principles and mechanisms of action of diagnostic devices engineered from bio-inspired

[*]**Correspondence to-** Mohiuddin Quadir, 701-231-6283, mohiuddin.quadir@ndus.edu.

Author role and conflict of Interest Statement: All authors contributed to writing and proof-reading of the manuscript. J.K. is associated with Actorius. Neither J.K. nor Actorius has competing interest with materials systems described in the project. Other authors do not have competing interests.

materials, describe current advances, and discuss future trends of the field, particularly in the context of cancer.

Keywords

Wearable devices; Biosensors; Nanotechnology; Cancer; Early detection

1. INTRODUCTION.

Wearable diagnostics and biosensors (WDBs) illustrate the efforts of the biomedical research community to miniaturize technologies for detecting and monitoring disease processes. Engineered with capabilities to identify patho-physiological anomalies in 'plug and play' basis, these devices not only reduce the complicacies and economic burden of any disease screening processes, but also increases user compliance significantly. In addition, WDBs provide opportunity to integrate with various early detection modalities to design point-of-care (POC) platforms. In fact, one of the major motivations towards the development of wearable diagnostic and biosensors stems from the demand to develop POC systems, which can function robustly in a low-resource settings. The socioeconomics of twentieth century also pushed the boundary of WDBs. Change of lifestyle, increase in health awareness, and need for speed for early diagnostic readouts also propelled the science and technologies of WDBs to its current state. Over last several years, a significant amount of contributions in WDB-research resulted in their cost-effective availability and production[1]. Advancement in chemical biology tools and techniques, microfluidics, emergence of lab-on-a-chip systems, 3D printing, genomics and parallel computing further fueled the development of WDBs. Materials science and engineering played significant roles in developing soft, stretchable, and biocompatible materials and electroactive substrates that can house the core technologies of WDBs, such as a liquid electrode, a microfluidic chip, or a flexible electroactive polymer. One of the breakthroughs with WDB development stem from innovation in *bio-inspired materials*, and bio-mimicking technologies. Such materials and approaches not only improved the efficiency and precision for detecting biological signals, but also provided with flexibility to construct WDBs of newer forms and functions. Thus, the era of WBD has been shaped and formed from the development of novel, natural or semi-synthetic bio-inspired materials capable of detecting an analyte of interest with accuracy and precision. In this review, we tend to identify the past, present, and future of bio-inspired materials used for WDBs, with a particular focus on cancer.

2. Rationale and Concept map of this review.

One of our driving forces to select cancer as the focus area of this review is because still there is a relative scarcity of sensitive detection technologies for the disease. An estimated new cancer cases of 1,898,160 and cancer deaths of 608,570 patients have been projected to occur in the United States in 2021[2]. Expenditure associated with cancer treatment is excruciatingly high for a huge segment of population. Cost for caring of cancer is ever-increasing – in 2020, the National costs for cancer care were estimated to be $208.9 billion in 2020. These estimates include costs associated with medical services and oral prescription

drugs[3]. With developmental surge of POC diagnostics for cancer, it can be expected that the cost of treatment can be suppressed if early detection capacity is increased. Thus, we divide this review into four sections, each of which deals with fundamental aspects of WDBs for cancer. First, we discuss the basic mechanics of WDBs with bio-inspiration as core-design principles. Detection and amplification of a disease-associated signal are fundamental features for most of the currently developed WDBs. Therefore, next we discuss the advances in signal detection and amplification technologies and feedback circuitry used in WDBs in the context of bio-inspired systems. Since the devices are wearable, a great stretch of opportunity lies in matching the conformation of the materials with human anatomy using 3D printing. Thus, we describe material design which are suitable for fabrication of WDBs using advanced manufacturing methods. Finally, we will identify how materials properties can be coupled to a particular bio- and pathological processes associated with cancer for rational designing of WDBs. Lastly, we aim to identify future trends of WDBs in detecting genetic signatures of diseases using the ‘Omics’ platforms.

3. Basic characteristics and design of WDBs.

Wearable diagnostics and biosensors can be classified as POC testing devices. The World Health Organization (WHO) focuses on following criteria for portable POC testing devices: (a) affordability (b) sensitivity, (c) specificity (d) compliance (measurements can be conducted in few steps with minimal training) (e) speed (results available in < 30 min) and robustness (f) equipment-free setup, and (g) deliverable to the end-users[1]. Wearable electronics are usually defined as self-sustaining electronic devices that can be worn on human body or loaded onto clothing. Generally, a biosensor is the integrated core module of a wearable device. A typical biosensor has been categorized into two basic units: an artificial or semisynthetic ‘bioreceptor’ coupled to a physico-chemical transducer. The bioreceptor usually interacts with biological targets (fluid, enzyme, or macromolecules, such as DNA) with substantial selectivity and specificity. The bioreceptor provides the interaction output in the form of electrochemical or mechanical signal to a transducer, which converts such input into a readable signal. Of note, bio-inspired materials can be used to fabricate any one of the abovementioned components of WDBs, improving their capacity to interact with targets or amplifying the readouts. One of the frequently-used, household example of bio-sensing and biorecognition is blood-glucose test strips. The basic operating principle for WDBs relies upon multiplexing of analyte detection with high sensitivity and specificity. Plethora of biological targets have been used as the source of biological analytes, which include but not limited to different types of body fluids, such as sweat, tears, saliva, and interstitial fluid (ISF). This is because the fluids can be collected in a noninvasive manner. Sensors for WDBs use different biological tissues (such as skin, organs, eyes) for analyte sources. The following sections describe different components of WDBs, which when integrated in the form of biosensors, can efficiently read the presence and amount of different analytes of interest required for detection and diagnosis of cancer.

4. Circuitry, data generation and read-out of a lab-on-a-chip (LOC) type biosensor.

As of now, most of the diagnostic screenings and tests are conducted in hospital-based laboratories, where expensive equipment is being used for diagnosis with trained personnel. Therefore, POC testing-based diagnostic tools and technologies are gaining traction because of their ease of operation and low maintenance. As the test procedures are significantly simplified, POC testing platforms significantly reduce the overall costs associated with equipment or personnel[4]. The advances in biosensor and "lab-on-a-chip" (LOC) technologies resulted in the ensemble of several POC testing modalities, which are portable and usable by patients or onsite by medical staffs. Fundamental characteristics of POC testing devices involve real-time data processing, ease of use, robustness, cost reduction, and simplicity of sample processing and preparation. To satisfy the above-mentioned criteria, the circuitry and mechanical design of WDBs needs to be compact and robust, and read-out must be fast and precise. This section will discuss the overview of WDBs and biosensors, and their general mechanism of signal transduction and power supply.

4.1. Electronic Construct of Biosensors:

4.1.1. Principles of analyte recognition.—As mentioned earlier, a biosensor is a device which utilizes either biological entities, such as enzyme, nucleic acid, and antibody as analytes, or it can measure overall anomaly of biochemical status of the body as signature stimuli. As biochemical signature, a biosensor can identify alteration of pH, electrolyte, or temperature of any physiological entities, such as blood, extracellular fluids, urine etc. The detection signal is then transformed into electrical signals through a transducer, which is measured afterwards through an appropriate readout. Therefore, the biosensor has three main components, i.e., a biorecognition element, a transducer and a signal display or read-out module. For example, in an antigen-antibody type classical biorecognition process, the recognition event involves interaction between the substrate-bound antibody with their cognate antigen. The transducer converts the analyte interactions into a quantifiable signal, so that the readout can show the specific signal generated by such interactions (Figure 1A)[5]. The first biosensor was developed in 1962 by Clark and Lyons, which essentially is an enzyme electrode. Its function was to monitor the oxygen in blood through coupling the glucose oxide with an amperometric electrode[6]. Since the advent of these earlier biosensors, numerous disease modification has been reported. Broadly, biosensors are categorized in different groups based on the transduction processes or the sensing components as shown in Figure 1B [7]. For example, considering different biological sensing elements such as enzymes, cells, tissues, antibodies, nucleic acids etc., biosensors can be classified as catalytic or affinity biosensors. The different types of physiological changes derived from the sensing receptors trigger the transduction process, where the transduction systems can be categorized as optical, electrochemical, piezoelectric and calorimetric transducers which are discussed in the next section.

4.1.2 Signal Transduction in Biosensors.—The selectivity of a biosensor is dependent on the biorecognition element. There are different transduction approaches to

generate signals in biosensors. Many of these approaches use optical inputs while the others are based on electrochemical and piezoelectric systems. In optics-based transduction, transducers collect information about an analyte via photons when the target analyte interacts with the biorecognition elements of WDBs. Here, photodetector is used to measure the variations of molecules in terms of concentration, mass or number and then transformed these variations into electrical signals[8, 9]. In electrochemical systems, electric current transfer within sensing electrodes as a result of electrochemical reactions are used as transduction element. Read-out signals can also be produced by generation of potential or charge storage (as potentiometric biosensor), measurement of current (as amperometric biosensor), conductance measurement (conductimetric) or resistance measurement and via fluctuation in capacitance (impedimetric biosensor) within electrodes. Electrochemical biosensors are composed of three electrodes, such as a reference electrode, a working electrode, and a counter electrode[7]. Sensing technologies using electrochemical processes showed potential application for cancer biomarker detection[10]. In piezoelectric systems electric signal is generated by pressure. Piezoelectric materials are coated with thin layer of conductive materials such as silver. Therefore, when a stress is applied, the ions in the materials move towards one of the conducting surfaces which results in flow of electric charge. There is another transduction process called calorimetric transducers, where changes in temperature results from a biochemical reaction that is measured with a thermistor[11].

4.3. Power Supply of Biosensors.

To detect any biomarkers, data processing, and output delivery via on- or offline mode, a source of power supply to sensors will be required. Therefore, self-powered sensors are highly popular for WDB design. The generation of power can be acquired from patho-physiological events, or from the environment like solar cells[12]. In human body, biofluids such as sweat can collected for generation of electrical energy[13, 14]. Body temperature is another source that can be utilized as thermogenerator[15]. Piezoelectric nanogenerators (PENGs) and electromagnetic nanogenerators (ENGs) can convert the mechanical movements of human body into electrical energy[16, 17]. In literature, a combination of these energy harvesting technologies is prevalent. For example, a triboelectric nanogenerators (TENGs) integrated with supercapacitor (SC) have been reported for generation of electrical energy for self-powered sensors[18]. Here, solar cells are used to generate electrical energy, which is stored in TENGs and SCs, and is harnessed to convert the mechanical energy of the human body into electrical energy.

5. Lab-on-a-Chip type Biosensors for Cancer detection.

In this section, we will focus on the recent development of biosensors and “lab-on-a-chip” (LOC) technologies as POC testing platforms for cancer patients. Yildiz et al. proposed an LOC- prototype, termed as MiSens, which have the potential to test cancer biomarkers[19]. The authors developed a new biochip which was integrated with microfluidic systems along with a real-time amperometric sensing that acted upon the interaction with an enzyme substrate. The authors also designed a docking station, where sensors can be easily docked through plug and play supports. This prototype has been used in the detection of prostate-specific antigen (PSA), a serum biomarker for the diagnosis and surveillance of prostate

cancer. Serum samples from clinical use were tested using the MiSens device and provided equivalent clinical results with standard testing devices, thus demonstrating a powerful approach of POC testing for prostate cancer. Parra-Cabrera et al. designed a novel lab-on-a-chip device which can simultaneously detect multiple biomarkers in prostate cancer by using simple voltage measurements[20]. This biosensing device consisted of gold electrodes, acting as voltage-based biosensors. These gold electrodes were arranged in a series array in a fluidic microchannel. The device also used two lateral microchannels to perform in-situ functionalization and sensing protocols. The fabrication has been done through photolithographic and cast molding techniques. The results from this device successfully quantified two proteins, namely, prostate-specific antigen (PSA) and spondin-2 (SPON2) which are usually found in blood, and when analyzed in combination, can be used for reliable detection of prostate cancer. Jiwei et al. designed a novel biosensor which can detect both PSA and alpha-methyl acyl-CoA racemase (AMACR) antigens from concentrated human serum[21]. Both PSA and AMACR are metabolic enzymes that has been showed to be highly expressed in prostate cancer cells and therefore can be used as biomarkers. The biosensing was carried out using differential pulse voltammetry. Authors concluded that relatively shorter period of time and very small quantity of test medium is capable of carrying out these experiments for significant amount of biomarker detection in prostate cancer. Akbari et al. proposed a sandwich typed electrode-based biosensor fabricated with reduced graphene oxide/gold nanoparticles (GO/AuNPs) to detect PSA[22]. The glassy carbon-based working electrode was electrochemically modified to GO/AuNPs in two steps, first polished the glassy carbon electrode with alumina powder, then GO/AuNPs/captured antibody (Ab_1) was dropped on the surface of electrode. This electrochemical sensor worked on the principle of single amplification and dual recognition strategy. Cyclic voltammetry and electrochemical impedance spectroscopy were used to measure the electrochemical properties during the analysis. Results showed that the biosensor showed high sensitivity towards the total and the free PSA. Indra et al. reported a new non-faradaic system - a lectin-assisted capacitive biosensor - to detect the prostate-specific membrane antigen (PSMA), which is an alternative to conventional biomarker, PSA, for determining prostate cancer[23]. Here, lectin was used as a bioreceptor for the direct detection of PSMA. The device utilized capacitive-based sensing, where the change in capacitance was solely originated from the dielectric changes, local conductance, and the charge distribution upon the biomolecular binding event on the transducer surface. In this study, aluminium interdigitated electrodes (IDEs) were used as transducers and was modified to form self-assembled monolayers (SAMs) comprised of carboxylate (-COOH) and thiol (or mercaptan, -SH) functional groups. Then carboxylic-functionalized gold nanoparticles (GNPs) were attached upon the SAM using Au-S bond interactions, to increase the conductivity along with the promotion of active conjugation of lectin. The latter was added as a molecule for specifically coupling with mannose present in PSMA. Finally, capacitive sensing was evaluated using Al-IDE to quantify the molecular binding event of lectin and PSMA. Here, GNP was utilized as signal amplifier with lectin in a capacitive sensor. Data showed that the device has a linear sensing range between 10 pM to 100 nM and accomplished the sensing threshold and sensitivity of 10 pM and 1.65 nF/pM respectively, which was comparable to the traditional sensing platforms. The first electrochemical and impedance-based biosensors that could detect PCA3 down to 0.128 nmol/L was developed by Juliana et al.[24]. These biosensors

were synthesized with the help of a layer of PCA3-complementary single-stranded DNA (ssDNA) probe, fabricated in a layer-by-layer (LbL) film pattern composed of chitosan (CHT) and carbon nanotubes (MWCNT). Therefore, the system was selective to PCA3 - a promising biomarker of prostate cancer. The authors confirmed the detection of PCA3 through impedance evaluation as well as via polarization-modulated infrared reflection absorption spectroscopy (PM-IRRAS). Table 1 summarizes a set of technologies relevant to different POC platforms proposed for detection of various cancers.

6. WDBs in Cancer Diagnostics and Therapy.

WDBs in cancer diagnostics have emerged as potential tools for early diagnosis, cancer therapy management, and real-time disease progression. WDBs such as adhesive patches, waist diapers, breast patches, and watch bands have been explored for the detection of skin cancer, prostate cancer, breast cancer, and other epithelial cancers, often times fabricated using bioinspired materials or designs.

Multiple WDBs are being developed to measure skin exposure to UV radiation and early diagnosis of skin cancer. Since 90% of non-melanoma skin cancers are associated with exposure to UV radiation from the sun, La Roche-Posay have developed stretchable electronic adhesive patches with the brand name, "*My UV Patch*" (Figure 2A)[25, 26]. Dimension of this transparent adhesive patch is of approximately one square inch in area and 50 micrometers thick. The ultrathin patch is layered and stretchable and consists of an electronically functional and a patterned photosensitive dye that responds to UV radiation. Further, the same manufacturer also developed the first portable electronic sensor without a battery that tracks the UV exposure, marketed as "*My Skin Track UV*" [27]. Attili et al. developed a WDB-based efficient therapeutic module for non-melanoma skin cancer. Their proposed WDB was based on ambulatory photodynamic therapy and consisted of a low-irradiating light source made up of an organic light-emitting diode (OLED). The OLED element composed of a flat, circular light-emitting area (2 cm in diameter) weighing 3 g. The OLED had aluminum foil backing on all four sides and the WDB was fixed with an adhesive tape to the patient (Figure 2B)[28]. Baskin et al. devised an oncomagnetic WDB. This device produced a treatment response when used in a patient with an untreatable left frontal glioblastoma (GBM)[29]. A 53-year-old patient showed reduced contrast-enhanced tumor (CET) volume with the treatment of this oncomagnetic device (Figure 2C and 2D). Bahrami et al. developed an ultra-wideband for cancer diagnosis. It utilizes single and dual-polarization antennas for wireless detection of breast cancer[30]. The antennas were 20 mm × 20 mm in dimension and operated at a frequency range of 2–4 GHz. A breast patch (iTBra) for early diagnosis of breast cancer (Figure 2E)[31] was developed by Cyrcadia Health and Nanyang Technological University (Singapore). The patch detected breast tissues for any circadian temperature changes. It is worn underneath clothes for a couple of hours per month, to detect variation in biological temperature of breast tissue. Conversely, Arcarisi et al. reported Palpreast, a new WDB for self-examination of breast and for early diagnosis of breast cancer (Figure 2F)[32]. The working principle of the WDB was based on a pressure sensing textile that is able to differentiate tissue stiffness, thus distinguishing between healthy and abnormal tissues. Teng et al. reported another WDB probe for uninterrupted monitoring of breast cancer neoadjuvant chemotherapy infusions[33]. The probe was based

on a near-infrared optical system, and the device was composed of a flexible printed circuit board that holds a paired arrangement of six dual-wavelength surface-mount LED and photodiode.

Researchers from Memorial Sloan Kettering Cancer Center developed an optical cancer detector in the form of a wrist band (Figure 3A)[34]. The wrist band can identify and distinguish multi-type cancer by identifying microRNA biomarkers circulating in bloodstream. Needle-like carbon nanotubes placed at key sites on the skin coupled with unique molecular biomarkers that are circulating in blood. The external wrist band consists of an infrared light emitter, wherein the infrared light is absorbed by nano-sensor implants and reemitted to an infrared light detector of the external wrist band. The measured signals calculated biomarker levels as an indicator of the cancer stage.

Capturing circulating tumor cells (CTCs) at high efficiency and precision will be a game changer in the area of liquid biopsy technologies for cancer. Hayes et al. described an *in vivo*, in dwelling intravascular aphaeretic WDBs for isolation of circulating tumor cells (CTC) through continuous CTC collection from a peripheral vein (Figure 3B)[35]. The WDB returned the remaining blood products after CTC enrichment. Thus, the WDB permitted interrogation of larger blood volumes than the traditional phlebotomy samples over a long duration. Table 2 provides a summary of the above-mentioned technologies usable for detection of different types of cancers.

7. Bioinspired Materials and Structures in designing WDBs and LOC Devices.

Classically, bio-inspiration encompasses the idea of development of novel materials, devices, and structures, that has been inspired by solutions found in biological systems[36]. Bioinspired devices are developed with materials of organic or inorganic origin, which can mimic the form, function, or conformational fluctuations of naturally occurring materials. Bioinspired materials and scaffolds have been used to detect physio-pathological conditions and do diagnostics such as drug screening, artificial tissue fabrication, and biosensing[37–39]. Before entering the area of cancer diagnostics, we would like to present an overarching theme of materials that have been selected routinely for constructing bio-inspired materials. A large plethora of such materials have been investigated for various diseases with variable success. Materials such as graphene, carbon nano dots, quantum dots, cellulose derivatives have long been used as materials candidates for preparation of WDBs. For example, Guo et al. developed a bioinspired framework structure with microcrack mechanosensory design as spiders and wing-locking sensing design as beetles [40]. In their work, the authors developed a microcrack mechanosensory structure using reduced graphene oxide (C-RGO) sheet layers. The C-RGO layers on elastic 3D polyurethane (PU) hydrophilic sponge systems (C-RGO@PU) was coated via supramolecular assembly of graphene oxide (GO) upon the modified PU sponge. To mimic wing-locking sensing design of beetles, polyaniline nanohair (PANIH) based conductive patterns were coated upon the surface of C-RGO sheet layers followed by an in situ oxidative polymerization. Finally, this conducting polymer (PANIH)-coated C-RGO sheet was layered upon the PU sponges (PANIH/C-RGO@PU).

This arrangement was used as pressure sensors. The sensors were used for monitoring the strain deformations with substantial flexibility (from 0.2% to 80%) and showed excellent sensitivity and prompt response/recovery time-period (22 ms/20 ms). Such properties could be usable to identify the early-stage Parkinson's disease (PD). Inspired by natural wing-locking capacity of beetles, this type of sensors is indeed a typical example of bioinspired design, and can be used for developing smart artificial electronic skins (E-skins) to monitor the pressure distribution, shape, and location of touch response in robotics.

Polyurethane (PU) and related high molecular weight of polymers have served as an attractive starting material for developing WDBs. Gao group reported a scale-like wearable substrate, which derived based on the principles of kirigami, combined with microfluidics and electronics[41]. The bioinspired stretchable sensor with wearability and biodegradation properties can help to collect sweat and perform diagnostic analysis along with motion monitoring. The end structure was composed of polyurethane (PU) and paper (cellulose) derived materials. This tunable scale sensor has different pattern of stretch length which helps to detect the applied strain for lactate, urea, uric acid sensing and motion sensing. The authors reported the fluctuation in resistance for stretching the scale like paper sensor and fluorescence enhancement resulting from sensing of lactic acid and urea from sweat. The sensor was composed of an integrated paper loaded with silica photonic crystal (PCs) and can be fabricated on regular office printing paper. One side of the paper was coated with conductive graphite and designed in kirigami style to generate a stretchable scale-like paper substrate, while the other side of the paper was designed for microfluidic channels with no carbon layer on this surface. Polyurethane (PU) strips was also attached on the paper from fish head-to-tail to support the elastic stretching and stability of the kirigami-styled paper design.

Hydrogels composed of natural polysaccharides, proteins, and cellulose are also interesting platforms for preparing bioinspired materials. Zhang et al[42] fabricated a chameleon skin-like bioinspired E-skin from modified cellulose hydrogel with addition of hydroxypropyl cellulose (HPC), thermo-responsive poly (acrylamide-co-acrylic acid) (PACA) and carbon nanotubes (CNTs). It was reported that HPC can be used to generate photonic liquid crystal structure and provide higher intensity colors for the responsive additives. Nanotubes were used to act as an enhancer of structural colors. This E-skin has cholesteric liquid-crystal nanostructure of HPCs along with the highly thermo-responsive PACA hydrogel component, which transmitted optical response from external stimuli such as temperature, mechanical pressure and tension fluctuation. The presence of CNT helped as a conductive material and reported the stimuli as a change of resistance. Overall, this flexible E-skin could not only report a stimuli through a resistance fluctuation, but also located the stimuli by via optical response.

Synthetic polymers such as poly (dimethylsiloxane), PDMS, and poly (vinylidiene fluoride), PVDF found versatile applicability to generate bioinspired structures. Recently, electrospun polymeric mats have been widely used for drug delivery, anti-cancer and various other biomedical applications[43, 44]. Inspired by plant leaves, a leaf venation (LV) skeleton structure was developed by Sun et al. These authors developed a tribologically-driven device with PDMS films using encapsulation layers, electrospun PVDF nanofiber mats, and a silver

nanowire network arrangement synthesized by green galvanic displacement reaction[45]. Silver nanowires have a low sheet resistance of 1.4 Ω sq^{-1} along with 82% transmittance and can increase up to 99% transmittance for sheet resistance of 68.2 Ω sq^{-1}. Using these fundamental properties, the developed nanodevice could detect physiological signals such as heartbeat, pulse, swallowing and neck tilting, and provided medical diagnostics and prediction of cardiovascular, esophagal and Parkinson's disease. The system acted as self-powering device, which harvested mechanical (triboelectric and piezoelectric mechanism) and thermal energies (pyroelectric mechanism) from body. The sensor could also monitor health condition during cold or flu using frequency, magnitude of voltage detected from coughing and breathing where mechanical and thermal energies were used as readouts.

Carbon-based materials with virtually limitless diversity in terms of molecular properties and arrangement, played a significant role in the fabrication of bioinspired diagnostic devices and biosensors. Guan et al. developed a graded, bioinspired nest-like architecture and detected enhancement of sensitivity and pressure due to the combined effect of the nest-like architecture and carbon black (CB) percolation network[46]. This 3D porous structure was designed based on ant nests and developed using the template method resulting in a network structure. This system can be used as flexible pressure sensor with high sensitivity and wide detection range of pressure fluctuation up to 1.2 MPa along with lower detection limit value of 20 Pa (rapid response time of 15ms with high stability above 10,000 loading and unloading cycle). The authors used conductive CB nanoparticles due to its active material properties, which aided to develop mechanical strength with large pressure loadings, promoted superior stability in percolation conductance, and enhanced uniform dispersion in a polymer matrix. This flexible sensor on human skin used to monitor physiological responses such as human breathing and wrist and jugular venous pulse (JVP). Due to its high sensitivity and low detection limit, this nest-like sensor device can be used as wearable diagnostic device with real-time monitoring facility.

Metallic nanoparticles have always been a great source of materials repository for designing bioinspired sensors. Inspired from tactile hairs in insect, Yin et al. developed bristled microparticles with zinc oxide (ZnO) microparticles that has high-aspect-ratio and density and acted as sensors[47]. This bioinspired sensor design was developed with particulate structures at micrometer scale range that were termed as 'sea urchin-shaped microparticles (SUSMs)'. These bioinspired bristled microparticles have high sensitivity for pressure and strain detection. The sensor could monitor respiratory fluctuation using air-pressure and track swallowing motion with superior sensitivity. Going from 3D to 2D materials, Shi et al. developed bioinspired microscale "brick-and-mortar" sensors based on nacre-mimetic architecture which showed high sensitivity, stretchability, and long term durability[48]. This nacre-mimetic architectures were derived as "brick" from the combination of 2D titanium carbide (Ti_3C_2Tx) MXene nanosheets and 1D silver nanowires. Such combination promoted high electrical conductivity and mechanical brittleness of the 'brick'. The 'mortar', on the other hand, was composed of poly (dopamine) (PDA)/ Ni^{2+}, which promoted toughening effects via enhancing interfacial interactions, increasing polymer chain stretching and stopping crack propagation. The sensors provided readout as motion signals during continuous movement and could track heart rate and other health-related activities. Hybrid systems, where natural materials encapsulated within synthetic

systems opened unforeseen possibility for designing bioinspired devices. Nawroth et al. fabricated bioinspired tissues using contractile muscle thin film techniques by mimicking the swimming process of jellyfish. The jellyfish medusa uses fast muscle contractions and slow muscle relaxations by an orchestrated organization of motor neurons and striated muscle[38, 49]. The authors developed the device by growing neonatal rat cardiomyocytes on the surface of a micropatterned polydimethylsiloxane (PDMS) polymer to form a bilayer "medusoid", which were successfully investigated for the thrust and feeding mechanism of jellyfish by evaluating stroke kinetics and animal-fluid interaction. This analysis could help to predict the physiological performance and perform diagnosis with reverse engineering of muscle. With these selected examples, we aim to rest the case that there is a virtually limitless possibility of using materials for bioinspired device design. In the following sections, we will focus on recent studies where such bioinspired materials and devices has been used for detection and treatment of cancer in point-of-care settings.

7.1. Synthetic Materials for Cancer Detection and Diagnostics.

Use of synthetic polymers for cancer detection and diagnosis has increased substantially in recent years. Capturing circulating cancer cells present in blood via bioinspired scaffolds have become an attractive platform of so-termed 'liquid biopsy'. For example, Wang et al. developed a pollen-like hierarchical substrate by mimicking the assembly process of pollen grains which provided specific distinguishable properties towards targeted cancer cells (Figure 4A and 4B)[50]. The authors constructed the device by assembling pollen grains of wild chrysanthemum in a pattern of closely packed layers. These pollen layers were arranged with the help of soft lithography technique, and the authors conducted a negative mimicking of pollen layers with polydimethylsiloxane (PDMS). The PDMS layer, which was loaded with curing agent, was deposited on dried pollen layers followed by crosslinking at elevated temperature. The 'positive replica' of pollen layers were designed with the help of 'negative replica' PDMS templates. Poly (methyl methacrylate), PMMA, along with UV curing agent was deposited upon the negative PDMS template followed by UV irradiation to solidify. These processes resulted in a pollen-like bio inspired hierarchical surfaces that was further functionalized with anti-EpCAM to recognize and isolate the cancer cells. Their work envisioned that this pollen-like device can be served as an early cancer detector. Dou et al. developed a bioinspired, hierarchical micro- and nanostructures by mimicking inner architecture of rose petals and implemented the system to capture circulating tumor cells (CTCs) using epithelial cell adhesion molecule antibodies (anti-EpCAM) as illustrated in Figure 4C and 4D [51]. As replicating polymer, PDMS was used and the liquid polymer was poured on rose petals, and disulfide functionalized petals generated micro- and nanostructures that were loaded with anti-EpCAM as specific recognition molecules to capture CTCs. These nanostructures showed higher capture efficiency of CTCs due to larger surface area and promoted enhanced surface interactions between cells and substrates. Disulfide bond was used for easy release of captured cells without triggering any cellular damages. Therefore, these scaffolds showed excellent capture efficiency and release of captured CTCs for further analysis.

Song et al. implemented a bioinspired system by replicating the mechanism of octopus to capture its prey and developed an aptamer functionalized nanosphere equipped microfluidic

chip (AP-Octopus-Chip), which was patterned in deterministic lateral displacement (DLD) arrangement for capturing cancer cells (Figure 5A and 5B)[52]. The authors replicated the tentacles of octopus by aptamer modification upon gold nanospheres (Au) for promoting better capture efficiency. This was achieved by using Anti-EpCAM Aptamer (SYL3C). The bioinspired device was fabricated by photolithography technique, PDMS casting, and functionalization of synthesized Au nanoparticles with thiolated aptamer SYL3C by freeze–thaw chemical modification. Au-SYL3C interface showed elevated capture efficiency and presence of thiol-gold bonding prevented the possible damage of the captured cells, which is crucial for post-capture genetic analysis of biological targets, i.e., CTCs in this instance.

For early detection of cancers, where the core detection principle hinges on identifying genetic and morphological identity of circulating tumor cells, it is critical that the captured cells sustain their cognate genetic or morphological signatures. Therefore, Dai et al. designed a bioinspired, conical micropattern on the PDMS substrate by replicating the wing structure of *beetle Coleoptera*. The micropattern was developed using two step nanoimprint lithography technique (Figure 6) [53]. The two major cytoskeletal components of fibroblast, actin and vimentin filament showed stable elongation with higher spreading area on conical micropattern PDMS substrate than flat PDMS. These bioinspired conical micropattern can promote the spreading and stability profile of target cells. Thus, the system can be applied for CTC capture that do not adversely affect the cells. Based on the study of cell attachment on patterned PDMS substrate, Liu et al. fabricated tumor-on-a-chip microfluidic system using soft lithography technique[54]. In this study microchannel mold was prepared on silicon substrate followed by pouring liquid PDMS polymer on the substrate. This fabrication method led to the formation of 3D microchannels on polymeric substrates[54], which can be used to investigate tumor evolution steps, experimenting on chemotherapy drugs, and possible anticancer therapy.

Polymer-based bioinspired materials have long been used for localized drug release and imaging for tumor location. Su et al. reported a near-infrared (NIR)-responsive bioinspired materials in which nanoparticles were camouflaged within RBC membranes for controlled release of drugs to treat metastatic breast cancer cells. In this design, the nanoparticles showed NIR-promoted cellular uptake[55]. The RBC replicate vesicle, which was separated from RBC membrane, was loaded with 1, 1-dioctadecyl-3, 3, 3, 3-tetramethylindotricarbocyanine iodide (DiR) cyanine dye. An anticancer drug, i.e., paclitaxel (PTX) was loaded within the designed poly (caprolactone)-ester end-capped polymeric nanoparticle cores. These polymeric cores were decorated with 1, 2-Dipalmitoyl-sn-glycero-3-phosphocholine-anchored Pluronic F68 to promote thermal sensitivity. This RBC-coated nanoparticles bypassed the immune response and supported prolonged circulation of the fluorescence probe. Irradiation of nanoparticle systems with NIR laser promoted DiR-induced hyperthermia, which enhanced tumor aggregation and broke the RBC membrane to disassemble the PTX-loaded nanoparticle. Such modular arrangement of nanoparticles within an RBC-membrane-bound capsules provided controllable drug release and uptake of tumor specific drug molecules. Such design could be used as the photothermal therapy (PTT) for metastatic breast cancer. Recently, Han et al. developed a biomimetic material with amphiphilic diblock copolymer poly (2-methacryloyloxyethyl phosphoryl choline)-b-Poly (n-butyl methacrylate) nanoparticles, which was synthesized using miniemulsion using

reversible addition-fragmentation chain transfer (RAFT) polymerization. The nanosystems were loaded with theranostic IR-780 dye for near infrared (NIR) imaging of, and PTT against cancer cells[56]. Versatility of polymeric materials design has also been used to deveop wearable devices for point-of-care cancer detection and diagnosis of cancer. Rahman et al. fabricated wearable bi-static radar system using flexible substrate of 5-(4-(perfluorohexyl) phenyl) thiophene-2-carbaldehyde as an antenna substrate for early detection of breast cancer[57]. The authors reported that the flexible device can promote uniform radiation flow with an average efficiency above 70%, with an average gain of above 1 dBi even at bending situation. This device was proposed for development of wearable, antenna-integrated bra for preliminary detection of breast cancer. Similarly, Teng et al. developed a stretchable, printed circuit board (PCB) with copper and polyimide for continuously evaluating hemodynamic activity for neoadjuvant chemotherapy infusions of breast cancer patient[33]. Performance of sensor system was evaluated with tissue-simulating phantoms and in-vivo participants. From the tissue-simulating phantom study and in-vivo participants, the research group reported that the sensor showed superior signal to noise ratio (SNR) along with the decrement of source-detector crosstalk, superior measurement accuracy, and high thermal stability. These wearable devices showed potential as platform for detecting prognostic hemodynamic fluctuation during chemotherapy in breast cancer patient.

7.2. Biobased materials – the new frontier.

Sustainability and accessibility of building blocks for designing advanced materials have also become an overarching theme for generating user-friendly, affordable biosensors and wearable devices. Biobased polymeric materials have surfaced in biomedical and pharmaceutical applications due to its ease of availability, low carbon footprint, unique biological features, and multi-functionality. Using multivalent, natural macromolecules as scaffold materials for WDB provided significant advantage in molecular recognition events. Recently, Bharathi et al. fabricated a bio-inspired nanocomposite from chitosan/copper oxide (CS-CuO) using a plant extracted bioflavonoid, Rutin (3, 3′, 4′, 5, 7-pentahydroxyflavone-3-rhamnoglucoside), which is extracted from tea, buckwheat, and apple plants[58, 59]. Rutin has anti-proliferative, and anti-carcinogenic functions[58, 60, 61]. CS-CuO nanocomposites with Rutin, showed concentration-promoted anti-proliferation effect against human lung cancer cells with increased apoptosis. Similarly, El Assal et al. recently reported biocompatible and bioinspired cryoprotectants with dextran and carboxylated ε-poly-L-lysine (CPLL) to conserve of human cytokine activated natural killer (NK) cell viability and effectiveness[62]. The NK cells, which represented as a frontline defense against cancers, were cryopreserved with slow freezing. After the thawing and removal of cryoprotective agents (CPAs), NK cells were preserved with dextran/CPLL media to sustain the viability of the cells from deterioration under the influence of toxic cryoprotectants. The group reported the maintenance of anti-tumor efficacy of the retrieved NK cells. Functional effectivity of retrieved NK cells was found to be superior against leukemia cells compared to control. This process showed an advantageous path of NK cell conservation without altering their cytotoxic strength for cancer immunotherapy. Such facile technology can indeed enhance applicability of immunotherapy under point-of-care setting, which is currently an unmet challenge. Zhong et al. reported cellulose nano-micelle derived from cellulose-graft-poly(p-dioxanone) (MCC-graft-PPDO) copolymer

loaded with three fluorescent conjugated polymers, namely, poly (9,9-dioctylfluoreny-2,7-diyl) (PFO), poly[2,7-(9,9-dihexylfluorene)-alt-4,7-(2,1,3-benzothiadiazole)] (PFBT) and poly [9,9-di(6-hexyl)-fluorene]-alt-co-[4,7-bis(thiophen-2-yl)-2,1,3-benzothiazole] (PFDBT) for cancer cells imaging[63]. Mansur et al. fabricated fluorescent alloyed-ZnCdS quantum dot (QD)-based core and biocompatible sodium carboxymethylcellulose (CMC)-based shells for cancer cell bio labeling for oncology applications. CMC-covered QDs were found to promote stabilization effects on the latter by forming metal polymer complex with polymer capping ligands [64]. Garg et al. developed bioinspired systems with heparin modified-cellulose acetate phthalate (HEC) nanoparticles to investigate cytotoxic effects of usnic acid (UA) following treatment to lung cancer cells[65]. The authors loaded anticancer compound UA in heparin-adipic acid-dihydrazide (ADH)- cellulose acetate phthalate (CAP) nanoparticles. This system showed controlled drug release from both HEC and CAP nanoparticle systems. The authors found that HEC nanoparticles demonstrated slower rate of release and enhanced hemocompatibility than those of CAP nanoparticles. UA-loaded HEC nanoparticles showed higher cytotoxicity compared to UA-loaded CAP nanoparticles and unencapsulated UA. Recently cellulose based nanomaterial was used in various of cancer cell treatment as it can entrap drug molecule via non-covalent interactions and also show controlled drug release properties [66]. Cellulose can also act as swellable polymer due to the presence of large number of hydroxyl groups. These hydroxyl groups also provide a suitable handle for chemical modifications [67]. Maier et al. developed a cellulose paper-based mask sensors integrated with two printed carbon-based electrodes to detect the electric fluctuation on change of moisture content during breathing. This cellulose derivative promoted the sensor to capture 10% of its weight of moisture[68]. Persian Blue (PB) was used in this paper device as it has high detection ability towards hydrogen peroxide (H_2O_2) which was generated from glucose oxidase, alkaline phosphatase, and horseradish peroxidase for labeling bioassay. Owing to the capacity of flexibility and stretchability, cellulose-based nanomaterials have higher possibility to fabricate bioinspired material and apply point-of-care treatment for cancer. Lee et al. fabricated a wearable, bioresorbable electronic patch (BEP) based on biodegradable polymers. The group used polylactic acid (PLA) (as encapsulate) and poly lactic-co-glycolic acid (PLGA) (as dielectric) in a multilayered device (Figure 7) [69]. These hydrophobic PLA layers protected a magnesium (Mg)-based wireless heating equipped sensors located in the core. Oxidized starch (OST) as hydrophilic layer, loaded with doxorubicin as chemotherapy drug, was attached to the layered sensor device. This arrangement of hydrophobic and hydrophilic segments enabled the device to stick to the localized tumor in Brain and provide sustained drug release. This device enabled the suppression of tumor volume and elevated survival rate in vivo.

7.3. Metal Nanoparticles and Complexes in Cancer Biosensing – Inspiration from Nature at Elemental Level.

Metal nanoparticle and its complexes are most common materials used for biosensor fabrication. As cancer detecting devices, An et al. fabricated an electrochemical biosensor made of benzoboric acid functionalized gold-plated PDMS substrate in a 3D patterned arrangement[70, 71]. Larger surface area of the arrangement played a crucial role for CTC capturing. Chen et al. investigated a coordination polymers composed of poly (2-methacryloyloxyethyl phosphoryl choline)-block-poly (serinyl acrylate) (PMPC-b-PserA).

The polymer design was inspired from amphoteric amino acids present in natural proteins[72]. Synthesized by reversible addition fragmentation chain transfer (RAFT) polymerization, the polymer product was able to encapsulate a hydrophobic molecule, curcumin. Interestingly, the assembled system was able to release curcumin at elevated deferoxamine (DFO) concentrations in acidic conditions. Such controlled encapsulation and release from protein-inspired synthetic polymeric assemblies were effective to inhibit breast cancer cells[72]. Ferric chloride ($FeCl_3$) was loaded within this polymer network as a as chelating agent. This was achieved via complexation of Fe^{3+} with poly (serinyl acrylate) at molar ratio of 3:1. Addition of DFO to an acidic system triggered the dissociation of drug-polymer assembly and released the curcumin. You et al. reported hybrid bioinspired gold nanoshells coated with bovine serum albumin (BSA)-functionalized gadolinium (Gd) and loaded with indocyanine green (ICG) as NIR absorbing phototherapeutic agent[73]. Considering the advantage of BSA−Gd for its longitudinal proton relaxivity and prolonged imaging time, this system promoted photothermal effect along with computed tomography (CT), photoacoustic (PA) and magnetic resonance imaging (MRI). Synergistic effect of photodynamic therapy (PDT) and PTT can be applied for imaging analysis of localized tumor cells. Chen et al. recently developed a bacterium-replicated metal organic frameworks (MOFs), which could mimic functional effects of Bacteria-mediated tumor therapy (BMTT) with nullifying the possible side effects, that can be used for cancer immunotherapy[74]. This bacteria-like spiky MOFs were synthesized by functionalization of aluminium (Al) sulfate with ruthenium (III) (Ru) chloride hydrate and organic linkers such as 2-aminoterephthalic acid. Salts of aluminum were used for promoting supplementary immunity by activating antigen presenting cells (APCs) and promote proliferation along with the activation of T cells[75]. Ruthenium metal complex was used as photothermal agents, which was activated via NIR[76]. This MOFs were injected in tumor locoregional area and irradiated with NIR laser which elevated the local temperature and recruited immune cells such as APCs and T cells due to presence of Al salts. Heat generation within the cancer tissue elevated the stress on cells which also activated the antitumor immunity. This biomimetic system showed a high efficacy in inhibiting tumor growth and declining the possibilities of recurrent growth of cancer cells and possible metastasis.

A bioinspired nanosystem was developed by Huang et al. using superparamagnetic iron oxide based modified nanoparticles, camouflaged within cancer cell membrane (CCM), to investigate cancer treatment through chemotherapy, hyperthermia therapy, and radiotherapy[77]. Doxorubicin (DOX) was added to poly (lysine) followed by functionalization with 3,3’-dithiobis sulfosuccinimidyl propionate (DTSSP) and amino group-modified superparamagnetic iron oxide nanoparticles (SPIO-NH_2) along with indocyanine (ICG) to fabricate nanoparticulate systems. Coating with CCM promoted nanoparticles to adhere to tumor cells and aggregate in the tumor locoregional area significantly compared to those accumulated in healthy tissue. Near-infrared (NIR) laser and X-ray irradiation promoted the release of DOX from cell membrane coated, modified iron oxide nanosystems. NIR laser and X-ray irradiation also promoted hyperthermia that aggravated tumor hypoxia and dampened radio resistance of the tumor. Huang et al’s result supported the possibility of taking advantage of autologous cancer cells from patients for designing multimodal cancer theranostics. Zhang et al. fabricated HeLa cancer cell

membrane disguised in zeolitic imidazolate framework 8 (ZIF-8) based MOF nanoparticles for carrying small interfering RNA to tumor to suppress PLK1 gene for lung cancer therapy[78]. This mechanism showed an efficient way to suppress cancer growth.

Gold nanoparticles have been used extensively as an attractive platform for biomedical applications. Mukherjee et al. studied gold nanoparticles biosynthesized using extract of *peltophorum pterocarpum* (PP) leaves and tagged with doxorubicin to design a drug delivery system[79]. This system promoted an effective inhibition of growth and proliferation of cancer cells cancer cells (A549, B16F10). Kim et al. reported $CuInS_2$/ZnS quantum dots system as tumor imaging system. The dots were conjugated with glycol-chitosan as coatings with the help of mercaptoundecanoic acid. The coated quantum dots were decorated with Arg-Gly-Asp (RGD) motif for binding to integrin receptors for in-vivo tumor targeting[80]. Hou et al. developed transferrin (Tf) conjugated hollow mesoporous CuS nanoparticles, loaded with iron dependent artesunate (AS) and synthesized nanoparticle systems for localized drug delivery, optical imaging, photoacoustic tomography, and immunofluorescence. These nanoparticles could be administered via peritumoral (PT) injection[81].

As a wearable device, Ciui et al. developed flexible bandage-based sensors for detection of skin melanoma (Figure 8)[82]. They have fabricated a flexible bandage with stretchable adhesive ink. The bandage was then coated with Ag/AgCl ink and polystyrene-block-polyisoprene-block-polystyrene (PS-PI-PS) based Ercon carbon ink layers followed by coating with an insulating layer. Such organized construct developed a dielectric separation of three electrode systems. Catechol-based gel solution was coated on the electrode surfaces using drop casting technique to form a biocompatible substrate. In the presence of the enzyme, tyrosinase (TYR), catechol (CAT) was oxidized to form benzoquinone (BQ) which was evaluated using the printed carbon and Ag/AgCl ink-based electrode, and the system can be used for early detection of skin cancer.

7.4. Emergence of 0 – 3D nanostructure in wearable diagnostics and biosensor design.

Nanoparticles with specific structural shapes promoted the functionality and activity of the bulk materials at nanoscale. Thus, nanostructures of different dimensions can be used for fabricating devices for cancer detection and diagnosis. Recently, Dong et al. fabricated bioinspired NanoVilli chip, which was synthesized by functionalizing silicon nanowire arrays in an arrangement inspired from unique structures of intestinal microvilli. The microvilli were decorated on PDMS substrate followed by functionalization with Anti-EpCAM biomarker to increase the system's efficiency for capturing tumor derived extracellular vesicles (EVs) from blood plasma (Figure 9A and 9B)[83]. The captured EVs was used for extracting RNA and analyzed through reverse transcription PCR. The approach could help predicting treatment effectiveness for lung cancer patients. Haslam et al. designed a label free graphene field effect transistor (GFET) immunosensors, which was synthesized using chemical vapor deposition (CVD) technique and developed on Si/SiO_2 substrate by photolithography assisted with evaporated chromium and gold sputtering. The sensors were functionalized with anti-hCG antibody on its surface to detect Human Chorionic Gonadotropin (hCG) glycoprotein for cancer cells[84]. Bioinspired designs have also been adopted from blood cells. He et al. fabricated bioinspired red

blood cell (RBC) membrane that disguised 2D Molybdenum diselenide ($MoSe_2$) nanosheets synthesized via liquid exfoliation techniques. Nanosheets were coated with RBC membrane for facilitating photothermal therapy (PTT) by stopping macrophage phagocytosis and enhancing hemocompatibility and circulation time[85]. This PTT technique with RBC-$MoSe_2$ showed strong advantages towards clinical use due to its in-vivo antitumor efficacy that is caused by triggering the immune system towards cancer cells. Zhang et al. fabricated a magneto-fluorescent system, fabricated from iron carbon quantum dots (FeN@CQDs) conjugated with folic acid and riboflavin. These nanostructures were incorporated into polymer nanospheres loaded with doxorubicin, to perform targeted drug release using imaging. The system was capable of working via PDT/PTT synergy against cancer cells via application of NIR irradiation[86]. Magneto-fluorescent sensors developed by Zhang et al., on the other hand, was fabricated by coating on single-walled carbon nanotubes (SWCNTs) with Fe_3O_4 conjugated carbon quantum dots (CQDs) through PEG linker, These sensors were also loaded with doxorubicin for targeted drug release and imaging for PDT and PTT applications against cancer cells[87]. Recently Wu et al. developed a novel bioinspired artificial tobacco mosaic virus (ATMV) by replicating unique rod like structure of tobacco mosaic virus (TMV)[88]. Strong tumor tissue tropism and oncolytic effectiveness were inherited with prolonged circulation of ATMVs. Such efficiency was clearly stemming from the bioinspired design of ATMVs that mimic the shielding, targeting, and arming tendencies of the oncolytic virus. The ATMVs showed high-aspect-ratio morphology along with stable and enhanced oncolytic efficacy, which promoted effective lysis due to breakdown of the membranes, endoplasmic reticulum disruption with Ca^{2+} release. In addition, ATMVs penetrated the neighboring infected cells and reach deep in tumor cells to start lysis. Single-walled carbon nanotube (SWNT) functionalized with RGD peptide was used to develop scaffolds for RNA, whereas capsid-subunit mimetic dendrons were designed with **π**–**π** stacking capacity onto the SWNT, which replicated the virus subunit arrays. Marangon et al. developed a dual system with multi-walled carbon nanotubes (MWCNT) arranged via **π**–**π** stacking and loaded with photosensitizer 5, 10, 15, 20-tetrakis (3-hydroxyphenyl) chlorin to form THPC/MWCNT system which could potentially used for PTT, PDT, and an integrated therapy[89, 90]. Xie et al. fabricated a SWCNT system using Evans Blue (EB) as dispersion agent for long circulation and promoted the system for fluorescent imaging as well as photodynamic therapy after loading with albumin conjugated fluorescent photosensitizer[91]. This albumin-CNT system promoted fluorescent and photoacoustic imaging of tumors for PDT and PTT and produced strong tumor ablation effect. Yin et al. developed tumor microenvironment (TME) responsive MnO_2 flakes coated and crosslinked on CNTs forming MnO_2/CNTs nanostructures, which were loaded with Chlorin e6 (Ce6) to synthesize Ce6-MnO_2/CNTs (CMCs) systems for PDT, PTT and fluorescence imaging on cancer cells[92]. MnO_2 was used for the reaction with endogenous H_2O_2 and H^+ to provide oxygen for Ce6 to generate cytotoxic oxygen ($^1O_2$) for enhancing PDT efficiency. Conjugating PEG to nanostructures has been an established platform, used by different research groups to manufacture bioinspired sensors. For example, Cao et al. fabricated a PEGylated nano-graphene oxide loaded with Chlorin e6 (GO-PEG-Ce6) system that can be excited at 660 nm and 808 nm, for PDT, PTT, or PDT/PTT integrated therapy followed by diffusion-weighted and blood oxygenation level dependent magnetic resonance imaging (MRI)[93]. Shim et al. developed Clostridium perfringens enterotoxin (CPE) loaded

with chlorin e6 (Ce6) separated by PEG spacers that was conjugated on the surface of reduced graphene oxide (rGO) to synthesize a rGO-based nanohybrid systems (CPC/rGO)[94]. The authors have compared this system to a conjugate of chlorin e6 (Ce6) with PEG spacer that was functionalized on the surface of rGO based system to yield PC/rGO architectures. Clearly, CPC/rGO system showed elevated cellular uptake in contrast to PC/rGO systems in claudin 4 overexpressing U87 glioblastoma cells. Following the irradiation at 660 and 808 nm that promoted generation of higher reactive oxygen compounds from CPC/rGO systems created significant elevation of temperature for PTT on cancer cells.

Orthogonally connecting several nanostructures is a viable strategy for designing bioinspired devices. Wang et al. fabricated a wearable origami paper based electrochemical epidermal growth factor receptor (EGFR), which was synthesized as nanocomposites via functionalization of amine groups of graphene with thionine (THI) and gold nanoparticles (AuNPs)(Figure 10A)[95, 96]. This nanocomposite was decorated with anti-EGFR to capture a specific type of cancer cells. The presence of graphene-based nanocomposites escalated the electron transfer rate along with elevated detection signal for higher accuracy. Similarly, Caccami et al. reported a graphene oxide-based wireless, wearable radiofrequency identification (RFID) sensors. These sensors were synthesized on the substrate of Si/SiO_2 with p-type doped silicon wafer and coated with rGO layer along with the gold as contact point between layers to regulate humidity and the temperature (Figure 10B and 10C)[97]. As GO has higher number of hydroxyl and carboxylic groups, further functionalization can be achieved through covalent conjugation to decorate different biomarkers on the substrate for early detection of cancer. Wang et al. fabricated an rGO-sunflower pollen (SFP) particles, which were spin coated on flexible PET substrate patterned with Au/Pt electrodes and decorated with anti-prostate specific antigen (anti-PSA) antibodies to identify the targeted cancer cells (Figure 10D)[98]. These 3D senor systems showed superior detection towards prostate specific antigen (PSA) compared to regular 2D graphene-coated sensors. As we found out in this section, synthetic polymers, nanoparticles, multidimensional nanostructures, and protein based nanosystems, all can function either alone or in combination with each other to enhance imaging and tracking capacity of diagnostic nanostructures and their usability. As such, these nanoscale products can open up the possibility of their inclusion into WDBs for cancer in clinical settings.

7.5. Protein based bioinspired nanosystems as sensors and diagnostics – closer to nature.

Proteins and polypeptides have always been a great source of bioinspiration for materials design. Damiati et al. developed bioinspired nanosystems based on bacterial surface layer protein (SbpA). Folate modified SbpA was grafted on gold substrate which was used as sensor for breast cancer detection with higher efficiency[99]. The bacterial protein, SbpA, was extracted from *Lysinibacillus sphaericus* CCM 2177 and functionalized with folic acid to synthesize SbpA-folate. This electrochemical sensor can differentiate between MCF-7 and HepG2 cancer cells. The sensor showed prominent advantages such as enhanced selectivity, sensitivity, and capture efficiency along with dimensional compatibility, for which it can be used as point-of-care sensor device. Stromal cells and extracellular matrix (ECM) harbor and protect cancer cells against deleterious effects of therapeutic nanoparticles,

thus disabling nanoparticle action. Tan et al. synthesized a bioinspired lipoprotein (bLP) loaded with photothermal agent $DiOC_{18}$ (7) (DiR) (D-bLP) and mertansine (M-bLP) – an anticancer drug which can promote efficient D-bLP penetration via moderate photothermia. The construed nanosystems can access cancer cells for antitumor treatment and showed suppression of metastasis[100]. The lipophilic DiR was used as photothermal agent for imaging whereas cytotoxic mertansine was used as anticancer drug for therapy. Bioinspired lipoproteins were synthesized with phospholipids of 1, 2-dimyristoyl-sn-glycero-3-phosphati-dylcholine (DMPC), 1, 2-dioleoyl-sn-glycero-3-phosphoethanola-mine (DOPE), and ApoA1-mimetic peptides.

Albumin, the most widely available plasma protein, has been an attractive platform that has been converted into bioinspired nanosystems. Recently, enzyme responsive albumin-based, gemcitabine (GEM) loaded delivery system was fabricated by Han et al. where the authors conjugated GEM to human serum albumin (HSA) through cathepsin B cleavable peptide GFLG and tagged the system with near-infrared (NIR) dye, IR780. The authors aim to synthesize HSA-GEM/IR780 nanoscale materials for chemotherapy and PTT [101]. Similarly, Sim et al. developed HSA nanoparticles loaded with melanin and paclitaxel (PTX) that showed efficient tumor chemotherapy with long circulation time[102]. Li et al. demonstrated HSA-based nanoparticles functionalized with Pt (IV) antitumor prodrug, NIR fluorophore, Cy5, and a quencher Qsy21 which enabled tumor cell imaging along with localized triggering of Pt(IV) prodrug, thus providing a theranostic effect[103]. Hu et al. reported a thermo-responsive reactive oxygen species (ROS) by functionalization of HSA-chlorin e6 nano-assemblies for use as a photodynamic therapy (PDT) against cancer cells[104]. Similarly, Chen et al. conjugated HSA with hemoglobin using disulfide bond to synthesize a hybrid protein oxygen carrier (HPOC) loaded with photosensitize chlorin e6 (Ce6) and formed C@HPOC which is used for PDT on cancer cells[105]. Ferritin protein-based systems also showed possible fabrication of bioinspired devices for cancer theranostics. Wang et al. reported fabrication of ultra-small copper sulfide (CuS) nanoparticles within the ferritin (Fn) nanocages through biomimetic synthesis. CuS-Fn nanocages responded with irradiation of NIR and promoted PTT for cancer theranostics[106]. This system showed superior photoacoustic tomography for quantitative ratiometric real time in-vivo photoacoustic imaging (PAI) of tumors. Superior PET imaging was also achievable with these systems due to presence of radionuclide ^{64}Cu as PET imaging agent. Currently clinically approved biomarkers such as anti-EpCAM antibody, transferrin, and pan-cytokeratins (CKs) 8, 18, 19 are widely used for capturing CTCs from cancer patients' blood samples which enables the early detection and further investigation of cancer cells[107]. The materials composed of 0–3D nanomaterials, synthetic polymers, and metal nanoparticles have shown variable level of success for cancer detection and diagnosis as summarized in Table 3.

8. Genomics aspect of Wearable devises and biosensor –challenges in the selection of biomarkers for bioinspired devices.

High throughput and multiplexed testing of captured bioanalytes for their cognate genetic signature can increase precision of detection and reduce off-target effects associated with disease diagnosis. Biological markers reflect cellular, biochemical as well as molecular

level fluctuations, which are detectable in different physiological compartments (tissues, cells, blood, and fluids). A wide variety of biomarkers like proteins (i.e., antigen or antibody) and nucleic acid (mutation in genomic DNA, micro-RNA) has been identified and routinely used for clinical diagnostics of different diseases including cancer using bioinspired sensors and devices. Compared to computer tomography and biopsy, biomarkers are more competitive tools for early diagnosis, therapeutic monitoring, and prognostic evaluation of cancer. However, selection of biomarkers, which sensors and wearable devices can identify or quantify, is the first line of challenge for devising a bioinspired system for genetic diagnosis. For example, with prostate cancer, which is the second most frequently diagnosed cancer in men and the fifth leading cause of death worldwide, PSA is used as one of the definitive ways of disease detection via prostate biopsy[108]. This is because serum PSA is a gland-specific biomarker rather than a cancer-specific one. Therefore, multiparametric ultrasound (mpUS), multiparametric magnetic resonance imaging (mpMRI), and nuclear imaging (positron emission tomography, PET) are prompted for clinical management of prostate cancer diagnosis, staging, active surveillance, and recurrence monitoring [109]. Healy et al concluded that PSA can be used as markers for biosensing for detection of prostate cancer in forensic samples. Although, this detection strategy has low detection limit (in the region of 0.05–0.005 ng/ml), reliability and high throughput, only sophisticated laboratories can process the analysis, causing delay in patient management and higher processing cost[110]. Therefore, different ultrasound imaging methods have been developed, and cancer detection can be improved by different algorithms. For breast cancer in general, ultrasound imaging, a noninvasive method, can detect tumor in dense breast which can be missed by mammography[111–113]. Coupling of bioinspired systems with these imaging modalities can bring significant changes in cancer detection.

Outside of imaging realm as diagnostic tools, Han et Al. explored the contribution of physiologically occuring, circulating tumor DNA (ctDNA) as biomarkers for sensing and diagnosis of cancer whether via conventional or bioinspired devices. Blood based ctDNA is considered over traditional physical and biochemical methods as it is non-invasive and show high specificity and sensitivity, thereby providing personalized snapshot of the disease. Limitations of ctDNA as biomarkers involve low signal-to-noise ratio, lack of colocalization, protein expression, and functional studies[114]. Huang et al. reported a protein array-based biomarker discovery in cancer detection[115]. Protein arrays provided immense advantages along with elevated throughput, and sensitive detection over last decades, thus offered excellent platforms for cancer proteomics research. There are three types of protein arrays i.e., analytical, functional, and reverse phase arrays. Protein arrays are continually evolving techniques, and if successfully combined with bioinspired materials, can bring in immense advantages along with elevated throughput, and sensitive detections of proteomic anomalies [115].

Micro-RNA (miRNA) is an elegant physiologically-relevant biomarker that is currently receiving traction as precision bioanalytes. Li et al. developed a method to detect low content of miRNA-21 with a sensor chip based on bioinspired photonic crystals in co-operation with cyclic enzymatic amplification method, providing the opportunity to detect breast cancer at early stage. This new sensor chip can extract RNA from cells that renders it potential for POC-setting for preliminary diagnosis of different diseases including

cancer. The technique can isolate miRNA-21 with a detection threshold of 55 fM and employed biocompatible polydopamine nanospheres (PDANs) and DNase I to construct a target-recycling multiplication routes on the photonic crystal. The advantage of this sensor chip is that the output fluorescence signal can be magnified particularly and amplification time is short[116].

Not only for diagnosis, but several bioinspired biosensors also been developed to assist cancer surgery. Blair et al. worked on the bioinspired biosensor-assisted surgery[117]. A six-channel color/near-infrared image sensor was used, mimicking the mantis shrimp visual systems, which will assist near-infrared fluorescence image guidance during the surgical procedure. In human prostate tumor this sensor can detect two tumor targeted fluorophores that can differentiate between tumor vs normal cells. In case of breast cancer, it can assist sentinel lymph node mapping using clinically approved near-infrared fluorophores during surgical resection. This biologically mimicking sensor has simple and compact structure that has flexible and better performance[117].

Gene mapping technology and machine learning are opening newer frontiers for precision medicine and disease diagnosis that can involve bioinspired technologies. Sun et al. used the gene mapping technology of the cancer genomics to develop the precision medicine in individualized manner. The approach needed the whole human genome sequence which was mapped back in 1990 and showed about 88 million common genetic variations including single nucleotide polymorphisms, insertions/deletions, and structural variants. Precision medicine usually employs fragments of disease related peptides to train immune cells to isolate target cells[118]. Mishra et al. discussed about the salivary cancer diagnostic approaches using biosensors and bioelectronics. Several of the major causes of cancer is genetic instability, modification, and DNA methylation. Saliva is a convenient source for collection of biomarkers for genotypting for diagnostic purpose as it is readily accessible in non-invasive manner. Although, saliva contains lower concentration of biomarker compared to serum in blood, the quantity of DNA found in saliva is usually enough for chip-based genotyping. The mean value of saliva DNA and serum DNA according to A260/A280 absorbance ratio is 1.56 and 1.71 respectively. DNA oxidation produces 8-hydroxy-2’deocyguanosine (8-OHdG) that can be used as a cancer biomarker, for example in acute leukemia of children, the urinary 8-OHdG is quantitatively analyzed. It was observed experimentally that, urinary 8-OHdG level is higher in patients with leukemia. Similarly, in head and neck squamous cell carcinoma (HNSC), the utilization of multiplex of salivary genomic biomarkers (TP53, PIK3CA, CDKN2A, FBXW7, HRAS, and NRAS) has investigated[119]. Salivary quantity of biomarkers, such as mitochondrial DNA (mtDNA) cytochrome C oxidase I (cox I) and cytochrome C oxidase II (cox II), can also act as biomarkers for identifying the prognosis of cancer after a specific procedure, for example post-operative radiation therapy[120]. It was also reported that the mitochondrial DNA can be correlated to tumor progression[12]. These salivary analytes are easy to detect via electrochemical methods, as well as by optical analysis, such as using surface enhanced Raman spectroscopy (SERS), fluorescence labeling, and by microfluidics[121].

9. Translation of WDBs, LOC Sensors and Detection Kits to Clinical Settings: Cancer and other diseases:

United States Food and Drug Administration (US FDA) approved many in vitro detection kit and imaging tools as companion diagnostic devices for cancer[122]. Table 4 represented several FDA approved, in vivo WDB devices, sensors and detection kits used for cancer diagnosis[123–129].

Other than cancer, WDBs have been employed for detection of many diseases. For example, WDBs for blood component monitoring can directly impact clinical decision-making and is useful for patients and for management of blood-related diseases. In addition, the blood components have found a direct correlation with biomarkers present in saliva and eccrine sweat. Towards this, external WDBs have been explored to detect blood glucose, sodium, chloride, potassium, and lactate by using saliva and sweat sensors. Gao et al. devised an epidermal WDB on a poly(ethylene terephthalate) substrate for the concurrent and constant detection of lactate and glucose[130]. The team demonstrated a mechanically versatile and completely integrated sensor for *in situ* sweat evaluation platform, which precisely detected electrolytes (potassium and sodium ions) and perspiration metabolites (lactate and glucose). Abellan-Llobregat et al, reported the fabrication of a printable and highly stretchable WDB based on platinum (Pt)-decorated graphite for sweat glucose detection (Figure 11)[131].

Glucose has been measured by using the electrode to measure the decrease of hydrogen peroxide by chrono-amperometry by immobilizing glucose oxidase on Pt-decorated graphite. This WDB was tested on human perspiration samples and showed a strong correlation between glucose concentration in perspiration and in blood. Continues Glucose Monitoring (CGM) sensor detects blood glucose level through interstitial fluid analysis. Dexcom® G5 and Eversense® E3 are US-FDA-approved continuous glucose monitors. Eversense® has been the first FDA-approved continuous glucose monitor that includes an entirely implantable sensor to track glucose levels and can be used for three months[132]. Koh et al. demonstrated a closed microfluidic WDB that readily harvested sweat from the pores to estimate lactate, glucose, hydronium ions (pH), and chloride[133]. The microfluidic system is comprised of a polydimethylsiloxane (PDMS) layer at the bottom of 500 μm, patterned with the required geometry with uniform 300 μm depth, and filled with colorimetric analysis reagents. The sensor was flexible and stretchable and could adhere to multiple parts of the body without any chemical or physical reaction by using soft device mechanics, biocompatible adhesives, and water-tight interfaces. The device passed sweat to the four channels to allow the simultaneous detection of the biomarkers. Bariya et al. fabricated roll-to-roll (R2R) gravure decorated electrochemical electrodes on 150 m stretchable PET substrate for the measurement of pH, potassium, sodium, glucose, and caffeine[134]. A 3 mm-diameter sensor on the device gets access to a few microlitres of fresh sweat every few minutes, representing sufficient fluid volume for stable and near real-time readings. Brolis Sensor Technology is developing a non-invasive wearable sensor to remotely test the concentration of blood elements such as glucose, ketones, lactate, urea, or ethanol[135]. The WDB uses ultra-compact laser-based integrated sensor technology for multi-molecule sensing throughout the entire bloodstream. Different type of WDBs developed for detecting

cardiovascular complications showed positive steps towards essential diagnostic care[136]. Several FDA approved devices are available for detection of various diseases are presented below (Table 5):

CONCLUSION

The foregoing discussion illustrates the transforming landscape of cancer diagnosis mediated via wearable devices and sensors, many of which use bioinspired design principles. We showed the basic construction of WDBs, and how bioinspired materials and processes have been incorporated within these WDBs for accurate and early detection of cancer. Although success of many of these devices are intrinsically connected to the types and pathology of the disease, it is obvious that with appropriately designed bio-inspired materials, it is possible to detect the pathological signature non-invasively from physiological samples at the early onset of the disease. Bio-inspiration propelled human curiosity since antiquity. Now the similar curiosity is catalyzing new discoveries that can combat debilitating diseases such as cancer. However, integration of bio-inspired materials into wearable devices and biosensors for cancer detection is a challenging task. Achieving this feat will need an integrated approach from materials scientists, chemists, engineers, and molecular biologist. Newer frontiers of bioinspired materials for cancer detection are constantly being explored, and nanometer-scale, autonomic, and feed-back regulated responsive systems are constantly pushing the boundary. With the advent of modern nanofabrication and characterization techniques, coupled with bioinformatics and machine-learning assisted capacity to detect anomalies at genetic level, we envision that the realm of bio-inspired materials for cancer detection and treatment is set to make a positive paradigm shift in foreseeable future.

ACKNOWLEDGEMENT

This research was supported by NIH grant number 1P20 GM109024 from the National Institute of General Medical Sciences (NIGMS) and U54GM128729 (DaCCoTA Cancer Collaborative on Translational Activity, Quadir). Partial support for this work was received from NSF grant no. IIA-1355466 from the North Dakota Established Program to Stimulate Competitive Research (ND-EPSCoR) through the Center for Sustainable Materials Science and NSF EPSCoR Track-1 Cooperative Agreement OIA # 1946202 (Quadir).

References:

1. Li P; Lee G-H; Kim SY; Kwon SY; Kim H-R; Park S, From Diagnosis to Treatment: Recent Advances in Patient-Friendly Biosensors and Implantable Devices. ACS Nano 2021, 15 (2), 1960–2004. [PubMed: 33534541]
2. Siegel RL; Miller KD; Fuchs HE; Jemal A, Cancer Statistics, 2021. CA: A Cancer Journal for Clinicians 2021, 71 (1), 7–33. [PubMed: 33433946]
3. Mariotto AB; Enewold L; Zhao J; Zeruto CA; Yabroff KR, Medical Care Costs Associated with Cancer Survivorship in the United States. Cancer Epidemiology Biomarkers & Prevention 2020, 29 (7), 1304.
4. Hayes B; Murphy C; Crawley A; O'Kennedy R, Developments in Point-of-Care Diagnostic Technology for Cancer Detection. Diagnostics (Basel) 2018, 8 (2), 39. [PubMed: 29865250]
5. Conroy PJ; Hearty S; Leonard P; O'Kennedy RJ, Antibody production, design and use for biosensor-based applications. Seminars in Cell & Developmental Biology 2009, 20 (1), 10–26. [PubMed: 19429487]
6. D'Orazio P, Biosensors in clinical chemistry. Clinica Chimica Acta 2003, 334 (1), 41–69.

7. Rodrigues D; Barbosa AI; Rebelo R; Kwon IK; Reis RL; Correlo VM, Skin-Integrated Wearable Systems and Implantable Biosensors: A Comprehensive Review. Biosensors 2020, 10 (7).
8. Hasan A; Nurunnabi M; Morshed M; Paul A; Polini A; Kuila T; Al Hariri M; Lee Y.-k.; Jaffa AA, Recent Advances in Application of Biosensors in Tissue Engineering. BioMed Research International 2014, 2014, 307519. [PubMed: 25165697]
9. Borisov SM; Wolfbeis OS, Optical Biosensors. Chemical Reviews 2008, 108 (2), 423–461. [PubMed: 18229952]
10. Islam MN; Channon RB, Chapter 1.3 - Electrochemical sensors. In Bioengineering Innovative Solutions for Cancer, Ladame S; Chang JYH, Eds. Academic Press: 2020; pp 47–71.
11. Perumal V; Hashim U, Advances in biosensors: Principle, architecture and applications. Journal of Applied Biomedicine 2014, 12 (1), 1–15.
12. Mondal S; Zehra N; Choudhury A; Iyer PK, Wearable Sensing Devices for Point of Care Diagnostics. ACS Applied Bio Materials 2021, 4 (1), 47–70.
13. Su Y; Wang J; Wang B; Yang T; Yang B; Xie G; Zhou Y; Zhang S; Tai H; Cai Z; Chen G; Jiang Y; Chen L-Q; Chen J, Alveolus-Inspired Active Membrane Sensors for Self-Powered Wearable Chemical Sensing and Breath Analysis. ACS Nano 2020, 14 (5), 6067–6075. [PubMed: 32271532]
14. Bandodkar AJ; You J-M; Kim N-H; Gu Y; Kumar R; Mohan AMV; Kurniawan J; Imani S; Nakagawa T; Parish B; Parthasarathy M; Mercier PP; Xu S; Wang J, Soft, stretchable, high power density electronic skin-based biofuel cells for scavenging energy from human sweat. Energy & Environmental Science 2017, 10 (7), 1581–1589.
15. Wang Y; Zhu W; Deng Y; Fu B; Zhu P; Yu Y; Li J; Guo J, Self-powered wearable pressure sensing system for continuous healthcare monitoring enabled by flexible thin-film thermoelectric generator. Nano Energy 2020, 73, 104773.
16. Zi Y; Lin L; Wang J; Wang S; Chen J; Fan X; Yang P-K; Yi F; Wang ZL, Triboelectric–Pyroelectric–Piezoelectric Hybrid Cell for High-Efficiency Energy-Harvesting and Self-Powered Sensing. Advanced Materials 2015, 27 (14), 2340–2347. [PubMed: 25727070]
17. Liu L; Yang X; Zhao L; Xu W; Wang J; Yang Q; Tang Q, Nanowrinkle-patterned flexible woven triboelectric nanogenerator toward self-powered wearable electronics. Nano Energy 2020, 73, 104797.
18. Wen Z; Yeh M-H; Guo H; Wang J; Zi Y; Xu W; Deng J; Zhu L; Wang X; Hu C; Zhu L; Sun X; Wang Zhong L, Self-powered textile for wearable electronics by hybridizing fiber-shaped nanogenerators, solar cells, and supercapacitors. Science Advances 2 (10), e1600097.
19. Uludag Y; Narter F; Sağlam E; Köktürk G; Gök MY; Akgün M; Barut S; Budak S, An integrated lab-on-a-chip-based electrochemical biosensor for rapid and sensitive detection of cancer biomarkers. Analytical and Bioanalytical Chemistry 2016, 408 (27), 7775–7783. [PubMed: 27562751]
20. Parra-Cabrera C; Samitier J; Homs-Corbera A, Multiple biomarkers biosensor with just-in-time functionalization: Application to prostate cancer detection. Biosensors and Bioelectronics 2016, 77, 1192–1200. [PubMed: 26590517]
21. Yao J; Wang Y; Dai Y; Liu CC, Bioconjugated, Single-Use Biosensor for the Detection of Biomarkers of Prostate Cancer. ACS Omega 2018, 3 (6), 6411–6418. [PubMed: 30023946]
22. Akbari Jonous Z; Shayeh JS; Yazdian F; Yadegari A; Hashemi M; Omidi M, An electrochemical biosensor for prostate cancer biomarker detection using graphene oxide-gold nanostructures. Engineering in Life Sciences 2019, 19 (3), 206–216. [PubMed: 32625003]
23. Subramani IG; Ayub RM; Gopinath SCB; Perumal V; Fathil MFM; Md Arshad MK, Lectin bioreceptor approach in capacitive biosensor for prostate-specific membrane antigen detection in diagnosing prostate cancer. Journal of the Taiwan Institute of Chemical Engineers 2021, 120, 9–16.
24. Soares JC; Soares AC; Rodrigues VC; Melendez ME; Santos AC; Faria EF; Reis RM; Carvalho AL; Oliveira ON, Detection of the Prostate Cancer Biomarker PCA3 with Electrochemical and Impedance-Based Biosensors. ACS Applied Materials & Interfaces 2019, 11 (50), 46645–46650. [PubMed: 31765118]

25. SHI Y; PIELAK R; BALOOCH G; L'OREAL; SHI Y; PIELAK R; BALOOCH G DEVICE AND SYSTEM FOR PERSONAL UV EXPOSURE MEASUREMENTS. WO/2017/120176, 2017-07-13, 2017.
26. Shi Y; Manco M; Moyal D; Huppert G; Araki H; Banks A; Joshi H; McKenzie R; Seewald A; Griffin G; Sen-Gupta E; Wright D; Bastien P; Valceschini F; Seité S; Wright JA; Ghaffari R; Rogers J; Balooch G; Pielak RM, Soft, stretchable, epidermal sensor with integrated electronics and photochemistry for measuring personal UV exposures. PLOS ONE 2018, 13 (1), e0190233. [PubMed: 29293664]
27. Laroche-Posay My Skin track UV. https://www.laroche-posay.me/en/article/MY-SKIN-TRACK-UV/a37392.aspx.
28. Attili SK; Lesar A; McNeill A; Camacho-Lopez M; Moseley H; Ibbotson S; Samuel IDW; Ferguson J, An open pilot study of ambulatory photodynamic therapy using a wearable low-irradiance organic light-emitting diode light source in the treatment of nonmelanoma skin cancer. British Journal of Dermatology 2009, 161 (1), 170–173. [PubMed: 19302071]
29. Baskin DS; Sharpe MA; Nguyen L; Helekar SA, Case Report: End-Stage Recurrent Glioblastoma Treated With a New Noninvasive Non-Contact Oncomagnetic Device. Front Oncol 2021, 11, 708017–708017. [PubMed: 34367992]
30. Bahramiabarghouei H; Porter E; Santorelli A; Gosselin B; Popović M; Rusch LA, Flexible 16 Antenna Array for Microwave Breast Cancer Detection. IEEE Transactions on Biomedical Engineering 2015, 62 (10), 2516–2525. [PubMed: 26011862]
31. Pramanik PKD; Upadhyaya BK; Pal S; Pal T, Chapter 1 - Internet of things, smart sensors, and pervasive systems: Enabling connected and pervasive healthcare. In Healthcare Data Analytics and Management, Dey N; Ashour AS; Bhatt C; James Fong S, Eds. Academic Press: 2019; pp 1–58.
32. Arcarisi L; Di Pietro L; Carbonaro N; Tognetti A; Ahluwalia A; De Maria C, Palpreast—A New Wearable Device for Breast Self-Examination. Applied Sciences 2019, 9 (3).
33. Fei T; Timothy C; Alexis S-B; Rachita C; Vivian EP; Raeef I; David AC; Samuel B; Naomi Yu K; Darren MR, Wearable near-infrared optical probe for continuous monitoring during breast cancer neoadjuvant chemotherapy infusions. Journal of Biomedical Optics 2017, 22 (1), 1–8.
34. MacRae M Wearable Cancer Monitors: Accessories to a Cure. https://aabme.asme.org/posts/wearable-cancer-monitors-accessories-to-a-cure.
35. Kim TH; Wang Y; Oliver CR; Thamm DH; Cooling L; Paoletti C; Smith KJ; Nagrath S; Hayes DF, A temporary indwelling intravascular aphaeretic system for in vivo enrichment of circulating tumor cells. Nature Communications 2019, 10 (1), 1478.
36. Sanchez C; Arribart H; Giraud Guille MM, Biomimetism and bioinspiration as tools for the design of innovative materials and systems. Nature Materials 2005, 4 (4), 277–288. [PubMed: 15875305]
37. Holley MT; Nagarajan N; Danielson C; Zorlutuna P; Park K, Development and characterization of muscle-based actuators for self-stabilizing swimming biorobots. Lab on a Chip 2016, 16 (18), 3473–3484. [PubMed: 27464463]
38. Clegg JR; Wagner AM; Shin SR; Hassan S; Khademhosseini A; Peppas NA, Modular fabrication of intelligent material-tissue interfaces for bioinspired and biomimetic devices. Progress in Materials Science 2019, 106, 100589. [PubMed: 32189815]
39. Park S-J; Gazzola M; Park KS; Park S; Di Santo V; Blevins EL; Lind JU; Campbell PH; Dauth S; Capulli AK; Pasqualini FS; Ahn S; Cho A; Yuan H; Maoz BM; Vijaykumar R; Choi J-W; Deisseroth K; Lauder GV; Mahadevan L; Parker KK, Phototactic guidance of a tissue-engineered soft-robotic ray. Science 2016, 353 (6295), 158. [PubMed: 27387948]
40. Guo Y; Guo Z; Zhong M; Wan P; Zhang W; Zhang L, A Flexible Wearable Pressure Sensor with Bioinspired Microcrack and Interlocking for Full-Range Human–Machine Interfacing. Small 2018, 14 (44), 1803018.
41. Gao B; Elbaz A; He Z; Xie Z; Xu H; Liu S; Su E; Liu H; Gu Z, Bioinspired Kirigami Fish-Based Highly Stretched Wearable Biosensor for Human Biochemical–Physiological Hybrid Monitoring. Advanced Materials Technologies 2018, 3 (4), 1700308.
42. Zhang Z; Chen Z; Wang Y; Zhao Y, Bioinspired conductive cellulose liquid-crystal hydrogels as multifunctional electrical skins. Proceedings of the National Academy of Sciences 2020, 117 (31), 18310–18316.

43. Cavo M; Serio F; Kale NR; D'Amone E; Gigli G; del Mercato LL, Electrospun nanofibers in cancer research: from engineering of in vitro 3D cancer models to therapy. Biomaterials Science 2020, 8 (18), 4887–4905. [PubMed: 32830832]
44. Gutschmidt D; Hazra RS; Zhou X; Xu X; Sabzi M; Jiang L, Electrospun, sepiolite-loaded poly(vinyl alcohol)/soy protein isolate nanofibers: Preparation, characterization, and their drug release behavior. International Journal of Pharmaceutics 2021, 594, 120172. [PubMed: 33321171]
45. Sun J-G; Yang T-N; Wang C-Y; Chen L-J, A flexible transparent one-structure tribo-piezo-pyroelectric hybrid energy generator based on bio-inspired silver nanowires network for biomechanical energy harvesting and physiological monitoring. Nano Energy 2018, 48, 383–390.
46. Guan X; Wang Z; Zhao W; Huang H; Wang S; Zhang Q; Zhong D; Lin W; Ding N; Peng Z, Flexible Piezoresistive Sensors with Wide-Range Pressure Measurements Based on a Graded Nest-like Architecture. ACS Applied Materials & Interfaces 2020, 12 (23), 26137–26144. [PubMed: 32423195]
47. Yin B; Liu X; Gao H; Fu T; Yao J, Bioinspired and bristled microparticles for ultrasensitive pressure and strain sensors. Nature Communications 2018, 9 (1).
48. Shi X; Wang H; Xie X; Xue Q; Zhang J; Kang S; Wang C; Liang J; Chen Y, Bioinspired Ultrasensitive and Stretchable MXene-Based Strain Sensor via Nacre-Mimetic Microscale "Brick-and-Mortar" Architecture. ACS Nano 2019, 13 (1), 649–659. [PubMed: 30566329]
49. Nawroth JC; Lee H; Feinberg AW; Ripplinger CM; McCain ML; Grosberg A; Dabiri JO; Parker KK, A tissue-engineered jellyfish with biomimetic propulsion. Nature Biotechnology 2012, 30 (8), 792–797.
50. Wang W; Yang G; Cui H; Meng J; Wang S; Jiang L, Bioinspired Pollen-Like Hierarchical Surface for Efficient Recognition of Target Cancer Cells. Advanced Healthcare Materials 2017, 6 (15), 1700003.
51. Dou X; Li P; Jiang S; Bayat H; Schönherr H, Bioinspired Hierarchically Structured Surfaces for Efficient Capture and Release of Circulating Tumor Cells. ACS Applied Materials & Interfaces 2017, 9 (10), 8508–8518. [PubMed: 28206737]
52. Song Y; Shi Y; Huang M; Wang W; Wang Y; Cheng J; Lei Z; Zhu Z; Yang C, Bioinspired Engineering of a Multivalent Aptamer-Functionalized Nanointerface to Enhance the Capture and Release of Circulating Tumor Cells. Angewandte Chemie International Edition 2019, 58 (8), 2236–2240. [PubMed: 30548959]
53. Dai J; Kong N; Lu Y; Yuan Y; Wu Q; Shi M; Zhang S; Wu Y; Peng W; Huang P; Chen X; Gong J; Yao Y, Bioinspired Conical Micropattern Modulates Cell Behaviors. ACS Applied Bio Materials 2018, 1 (5), 1416–1423.
54. Liu X; Fang J; Huang S; Wu X; Xie X; Wang J; Liu F; Zhang M; Peng Z; Hu N, Tumor-on-a-chip: from bioinspired design to biomedical application. Microsystems & Nanoengineering 2021, 7 (1), 50. [PubMed: 34567763]
55. Su J; Sun H; Meng Q; Yin Q; Zhang P; Zhang Z; Yu H; Li Y, Bioinspired Nanoparticles with NIR-Controlled Drug Release for Synergetic Chemophotothermal Therapy of Metastatic Breast Cancer. Advanced Functional Materials 2016, 26 (41), 7495–7506.
56. Han H; Zhang S; Wang Y; Chen T; Jin Q; Chen Y; Li Z; Ji J, Biomimetic drug nanocarriers prepared by miniemulsion polymerization for near-infrared imaging and photothermal therapy. Polymer 2016, 82, 255–261.
57. Rahman A; Islam MT; Singh MJ; Kibria S; Akhtaruzzaman M, Electromagnetic Performances Analysis of an Ultra-wideband and Flexible Material Antenna in Microwave Breast Imaging: To Implement A Wearable Medical Bra. Scientific Reports 2016, 6 (1), 38906. [PubMed: 28008923]
58. Bharathi D; Ranjithkumar R; Chandarshekar B; Bhuvaneshwari V, Bio-inspired synthesis of chitosan/copper oxide nanocomposite using rutin and their anti-proliferative activity in human lung cancer cells. International Journal of Biological Macromolecules 2019, 141, 476–483. [PubMed: 31473316]
59. Ahmed MM; Hussein MMA, Neurotoxic effects of silver nanoparticles and the protective role of rutin. Biomedicine & Pharmacotherapy 2017, 90, 731–739. [PubMed: 28419969]

60. Wu F; Chen J; Fan LM; Liu K; Zhang N; Li SW; Zhu H; Gao HC, Analysis of the effect of rutin on GSK-3β and TNF-α expression in lung cancer. Exp Ther Med 2017, 14 (1), 127–130. [PubMed: 28672902]
61. Gullón B; Lú-Chau TA; Moreira MT; Lema JM; Eibes G, Rutin: A review on extraction, identification and purification methods, biological activities and approaches to enhance its bioavailability. Trends in Food Science & Technology 2017, 67, 220–235.
62. El Assal R; Abou-Elkacem L; Tocchio A; Pasley S; Matosevic S; Kaplan DL; Zylberberg C; Demirci U, Bioinspired Preservation of Natural Killer Cells for Cancer Immunotherapy. Advanced Science 2019, 6 (6), 1802045. [PubMed: 30937270]
63. Zhong H; Zhang J; Guo Y; Wang L; Ge W; Chen M; Sun R; Wang X, Multi-color light-emitting amphiphilic cellulose/conjugated polymers nanomicelles for tumor cell imaging. Cellulose 2017, 24 (2), 889–902.
64. Mansur AAP; de Carvalho FG; Mansur RL; Carvalho SM; de Oliveira LC; Mansur HS, Carboxymethylcellulose/ZnCdS fluorescent quantum dot nanoconjugates for cancer cell bioimaging. International Journal of Biological Macromolecules 2017, 96, 675–686. [PubMed: 28049016]
65. Garg A; Sahu N; Yadav A, Usnic Acid-loaded Bioinspired Heparin Modified-cellulose Acetate Phthalate Nanoparticle(s) as an Efficient Carrier for Site-specific Delivery in Lung Cancer Cells. International Journal of Pharmaceutical Investigation 25 Sep. 2018 8(2):53–2.
66. Hazra RS; Dutta D; Mamnoon B; Nair G; Knight A; Mallik S; Ganai S; Reindl K; Jiang L; Quadir M, Polymeric Composite Matrix with High Biobased Content as Pharmaceutically Relevant Molecular Encapsulation and Release Platform. ACS Applied Materials & Interfaces 2021, 13 (34), 40229–40248. [PubMed: 34423963]
67. Hazra RS; Kale N; Aland G; Qayyumi B; Mitra D; Jiang L; Bajwa D; Khandare J; Chaturvedi P; Quadir M, Cellulose Mediated Transferrin Nanocages for Enumeration of Circulating Tumor Cells for Head and Neck Cancer. Scientific Reports 2020, 10 (1), 10010. [PubMed: 32561829]
68. Maier D; Laubender E; Basavanna A; Schumann S; Güder F; Urban GA; Dincer C, Toward Continuous Monitoring of Breath Biochemistry: A Paper-Based Wearable Sensor for Real-Time Hydrogen Peroxide Measurement in Simulated Breath. ACS Sensors 2019, 4 (11), 2945–2951. [PubMed: 31610653]
69. Lee J; Cho HR; Cha GD; Seo H; Lee S; Park C-K; Kim JW; Qiao S; Wang L; Kang D; Kang T; Ichikawa T; Kim J; Lee H; Lee W; Kim S; Lee S-T; Lu N; Hyeon T; Choi SH; Kim D-H, Flexible, sticky, and biodegradable wireless device for drug delivery to brain tumors. Nature Communications 2019, 10 (1), 5205.
70. An L; Wang G; Han Y; Li T; Jin P; Liu S, Electrochemical biosensor for cancer cell detection based on a surface 3D micro-array. Lab on a Chip 2018, 18 (2), 335–342. [PubMed: 29260185]
71. Pérez JAC; Sosa-Hernández JE; Hussain SM; Bilal M; Parra-Saldivar R; Iqbal HMN, Bioinspired biomaterials and enzyme-based biosensors for point-of-care applications with reference to cancer and bio-imaging. Biocatalysis and Agricultural Biotechnology 2019, 17, 168–176.
72. Chen P-C; Lai JJ; Huang C-J, Bio-Inspired Amphoteric Polymer for Triggered-Release Drug Delivery on Breast Cancer Cells Based on Metal Coordination. ACS Applied Materials & Interfaces 2021, 13 (22), 25663–25673. [PubMed: 34032419]
73. You Q; Sun Q; Yu M; Wang J; Wang S; Liu L; Cheng Y; Wang Y; Song Y; Tan F; Li N, BSA–Bioinspired Gadolinium Hybrid-Functionalized Hollow Gold Nanoshells for NIRF/PA/CT/MR Quadmodal Diagnostic Imaging-Guided Photothermal/Photodynamic Cancer Therapy. ACS Applied Materials & Interfaces 2017, 9 (46), 40017–40030. [PubMed: 29087183]
74. Chen P-M; Pan W-Y; Miao Y-B; Liu Y-M; Luo P-K; Phung HN; Wu W-W; Ting Y-H; Yeh C-Y; Chiang M-C; Chia W-T; Sung H-W, Bioinspired Engineering of a Bacterium-Like Metal–Organic Framework for Cancer Immunotherapy. Advanced Functional Materials 2020, 30 (42), 2003764.
75. Miao Y-B; Pan W-Y; Chen K-H; Wei H-J; Mi F-L; Lu M-Y; Chang Y; Sung H-W, Engineering a Nanoscale Al-MOF-Armored Antigen Carried by a “Trojan Horse”-Like Platform for Oral Vaccination to Induce Potent and Long-Lasting Immunity. Advanced Functional Materials 2019, 29 (43), 1904828.

76. Wang W-L; Guo Z; Lu Y; Shen X-C; Chen T; Huang R-T; Zhou B; Wen C; Liang H; Jiang B-P, Receptor-Mediated and Tumor-Microenvironment Combination-Responsive Ru Nanoaggregates for Enhanced Cancer Phototheranostics. ACS Applied Materials & Interfaces 2019, 11 (19), 17294–17305. [PubMed: 30977628]
77. Huang Y; Mei C; Tian Y; Nie T; Liu Z; Chen T, Bioinspired tumor-homing nanosystem for precise cancer therapy via reprogramming of tumor-associated macrophages. NPG Asia Materials 2018, 10 (10), 1002–1015.
78. Zhang Y; Yang L; Wang H; Huang J; Lin Y; Chen S; Guan X; Yi M; Li S; Zhang L, Bioinspired metal–organic frameworks mediated efficient delivery of siRNA for cancer therapy. Chemical Engineering Journal 2021, 426, 131926.
79. Mukherjee S; Sau S; Madhuri D; Bollu V; Madhusudana K; Sreedhar B; Banerjee R; Patra C, Green Synthesis and Characterization of Monodispersed Gold Nanoparticles: Toxicity Study, Delivery of Doxorubicin and Its Bio-Distribution in Mouse Model. J Biomed Nanotechnol. 2016 Jan, (12(1):165–81.). [PubMed: 27301182]
80. Kim E-M; Lim ST; Sohn M-H; Jeong H-J, Facile synthesis of near-infrared CuInS2/ZnS quantum dots and glycol-chitosan coating for in vivo imaging. Journal of Nanoparticle Research 2017, 19 (7), 251.
81. Hou L; Shan X; Hao L; Feng Q; Zhang Z, Copper sulfide nanoparticle-based localized drug delivery system as an effective cancer synergistic treatment and theranostic platform. Acta Biomaterialia 2017, 54, 307–320. [PubMed: 28274767]
82. Ciui B; Martin A; Mishra RK; Brunetti B; Nakagawa T; Dawkins TJ; Lyu M; Cristea C; Sandulescu R; Wang J, Wearable Wireless Tyrosinase Bandage and Microneedle Sensors: Toward Melanoma Screening. Advanced Healthcare Materials 2018, 7 (7), 1701264.
83. Dong J; Zhang RY; Sun N; Smalley M; Wu Z; Zhou A; Chou S-J; Jan YJ; Yang P; Bao L; Qi D; Tang X; Tseng P; Hua Y; Xu D; Kao R; Meng M; Zheng X; Liu Y; Vagner T; Chai X; Zhou D; Li M; Chiou S-H; Zheng G; Di Vizio D; Agopian VG; Posadas E; Jonas SJ; Ju S-P; Weiss PS; Zhao M; Tseng H-R; Zhu Y, Bio-Inspired NanoVilli Chips for Enhanced Capture of Tumor-Derived Extracellular Vesicles: Toward Non-Invasive Detection of Gene Alterations in Non-Small Cell Lung Cancer. ACS Applied Materials & Interfaces 2019, 11 (15), 13973–13983. [PubMed: 30892008]
84. Haslam C; Damiati S; Whitley T; Davey P; Ifeachor E; Awan SA, Label-Free Sensors Based on Graphene Field-Effect Transistors for the Detection of Human Chorionic Gonadotropin Cancer Risk Biomarker. Diagnostics 2018, 8 (1).
85. He L; Nie T; Xia X; Liu T; Huang Y; Wang X; Chen T, Designing Bioinspired 2D MoSe2 Nanosheet for Efficient Photothermal-Triggered Cancer Immunotherapy with Reprogramming Tumor-Associated Macrophages. Advanced Functional Materials 2019, 29 (30), 1901240.
86. Zhang M; Wang W; Zhou N; Yuan P; Su Y; Shao M; Chi C; Pan F, Near-infrared light triggered photo-therapy, in combination with chemotherapy using magnetofluorescent carbon quantum dots for effective cancer treating. Carbon 2017, 118, 752–764.
87. Zhang M; Wang W; Cui Y; Chu X; Sun B; Zhou N; Shen J, Magnetofluorescent Fe3O4/carbon quantum dots coated single-walled carbon nanotubes as dual-modal targeted imaging and chemo/photodynamic/photothermal triple-modal therapeutic agents. Chemical Engineering Journal 2018, 338, 526–538.
88. Wu H; Zhong D; Zhang Z; Li Y; Zhang X; Li Y; Zhang Z; Xu X; Yang J; Gu Z, Bioinspired Artificial Tobacco Mosaic Virus with Combined Oncolytic Properties to Completely Destroy Multidrug-Resistant Cancer. Advanced Materials 2020, 32 (9), 1904958.
89. Marangon I; Ménard-Moyon C; Silva AKA; Bianco A; Luciani N; Gazeau F, Synergic mechanisms of photothermal and photodynamic therapies mediated by photosensitizer/carbon nanotube complexes. Carbon 2016, 97, 110–123.
90. Dias LD; Mfouo-Tynga IS, Learning from Nature: Bioinspired Chlorin-Based Photosensitizers Immobilized on Carbon Materials for Combined Photodynamic and Photothermal Therapy. Biomimetics 2020, 5 (4).
91. Xie L; Wang G; Zhou H; Zhang F; Guo Z; Liu C; Zhang X; Zhu L, Functional long circulating single walled carbon nanotubes for fluorescent/photoacoustic imaging-guided enhanced phototherapy. Biomaterials 2016, 103, 219–228. [PubMed: 27392290]

92. Yin Z; Chen D; Zou J; Shao J; Tang H; Xu H; Si W; Dong X, Tumor Microenvironment Responsive Oxygen-Self-Generating Nanoplatform for Dual-Imaging Guided Photodynamic and Photothermal Therapy. ChemistrySelect 2018, 3 (16), 4366–4373.

93. Cao J; An H; Huang X; Fu G; Zhuang R; Zhu L; Xie J; Zhang F, Monitoring of the tumor response to nano-graphene oxide-mediated photothermal/photodynamic therapy by diffusion-weighted and BOLD MRI. Nanoscale 2016, 8 (19), 10152–10159. [PubMed: 27121639]

94. Shim G; Kim M-G; Jin H; Kim J; Oh Y-K, Claudin 4-targeted nanographene phototherapy using a Clostridium perfringens enterotoxin peptide-photosensitizer conjugate. Acta Pharmacologica Sinica 2017, 38 (6), 954–962. [PubMed: 28552914]

95. Wang Y; Sun S; Luo J; Xiong Y; Ming T; Liu J; Ma Y; Yan S; Yang Y; Yang Z; Reboud J; Yin H; Cooper JM; Cai X, Low sample volume origami-paper-based graphene-modified aptasensors for label-free electrochemical detection of cancer biomarker-EGFR. Microsystems & Nanoengineering 2020, 6 (1), 32. [PubMed: 34567646]

96. Baldo TA; De Lima LF; Mendes LF; De Araujo WR; Paixão TRLC; Coltro WKT, Wearable and Biodegradable Sensors for Clinical and Environmental Applications. ACS Applied Electronic Materials 2021, 3 (1), 68–100.

97. Caccami MC; Mulla MYS; Di Natale C; Marrocco G, Graphene oxide-based radiofrequency identification wearable sensor for breath monitoring. IET Microwaves, Antennas & Propagation 2018, 12 (4), 467–471.

98. Wang L; Jackman JA; Ng WB; Cho N-J, Flexible, Graphene-Coated Biocomposite for Highly Sensitive, Real-Time Molecular Detection. Advanced Functional Materials 2016, 26 (47), 8623–8630.

99. Damiati S; Peacock M; Mhanna R; Søpstad S; Sleytr UB; Schuster B, Bioinspired detection sensor based on functional nanostructures of S-proteins to target the folate receptors in breast cancer cells. Sensors and Actuators B: Chemical 2018, 267, 224–230.

100. Tan T; Hu H; Wang H; Li J; Wang Z; Wang J; Wang S; Zhang Z; Li Y, Bioinspired lipoproteins-mediated photothermia remodels tumor stroma to improve cancer cell accessibility of second nanoparticles. Nature Communications 2019, 10 (1).

101. Han H; Wang J; Chen T; Yin L; Jin Q; Ji J, Enzyme-sensitive gemcitabine conjugated albumin nanoparticles as a versatile theranostic nanoplatform for pancreatic cancer treatment. Journal of Colloid and Interface Science 2017, 507, 217–224. [PubMed: 28800445]

102. Sim C; Kim H; Moon H; Lee H; Chang JH; Kim H, Photoacoustic-based nanomedicine for cancer diagnosis and therapy. Journal of Controlled Release 2015, 203, 118–125. [PubMed: 25701310]

103. Li X; Mu J; Liu F; Tan EWP; Khezri B; Webster RD; Yeow EKL; Xing B, Human Transport Protein Carrier for Controlled Photoactivation of Antitumor Prodrug and Real-Time Intracellular Tumor Imaging. Bioconjugate Chemistry 2015, 26 (5), 955–961. [PubMed: 25938732]

104. Hu D; Sheng Z; Gao G; Siu F; Liu C; Wan Q; Gong P; Zheng H; Ma Y; Cai L, Activatable albumin-photosensitizer nanoassemblies for triple-modal imaging and thermal-modulated photodynamic therapy of cancer. Biomaterials 2016, 93, 10–19. [PubMed: 27061266]

105. Chen Z; Liu L; Liang R; Luo Z; He H; Wu Z; Tian H; Zheng M; Ma Y; Cai L, Bioinspired Hybrid Protein Oxygen Nanocarrier Amplified Photodynamic Therapy for Eliciting Anti-tumor Immunity and Abscopal Effect. ACS Nano 2018, 12 (8), 8633–8645. [PubMed: 30005164]

106. Wang Z; Huang P; Jacobson O; Wang Z; Liu Y; Lin L; Lin J; Lu N; Zhang H; Tian R; Niu G; Liu G; Chen X, Biomineralization-Inspired Synthesis of Copper Sulfide–Ferritin Nanocages as Cancer Theranostics. ACS Nano 2016, 10 (3), 3453–3460. [PubMed: 26871955]

107. Khandare J; Arora S; Singh B; D'Souza A; Singh N; Kale N; Bhide S; Ashturkar A; Vasudevan A; Aland G, Device for the enumeration and continuous removal of circulating tumor cells in improving overall survival of epithelial cancer patients. Journal of Clinical Oncology 2020, 38 (15_suppl), e15043–e15043.

108. Torre LA; Bray F; Siegel RL; Ferlay J; Lortet-Tieulent J; Jemal A, Global cancer statistics, 2012. CA: A Cancer Journal for Clinicians 2015, 65 (2), 87–108. [PubMed: 25651787]

109. Sarkar S; Das S, A Review of Imaging Methods for Prostate Cancer Detection. Biomed Eng Comput Biol 2016, 7 (Suppl 1), 1–15.

110. Healy DA; Hayes CJ; Leonard P; McKenna L; O'Kennedy R, Biosensor developments: application to prostate-specific antigen detection. Trends in Biotechnology 2007, 25 (3), 125–131. [PubMed: 17257699]
111. Ozmen N; Dapp R; Zapf M; Gemmeke H; Ruiter NV; Dongen K. W. A. v., Comparing different ultrasound imaging methods for breast cancer detection. IEEE Transactions on Ultrasonics, Ferroelectrics, and Frequency Control 2015, 62 (4), 637–646. [PubMed: 25881342]
112. Gordon PB; Goldenberg SL, Malignant breast masses detected only by ultrasound. A retrospective review. Cancer 1995, 76 (4), 626–630. [PubMed: 8625156]
113. Ying X; Lin Y; Xia X; Hu B; Zhu Z; He P, A Comparison of Mammography and Ultrasound in Women with Breast Disease: A Receiver Operating Characteristic Analysis. The Breast Journal 2012, 18 (2), 130–138. [PubMed: 22356352]
114. Han X; Wang J; Sun Y, Circulating Tumor DNA as Biomarkers for Cancer Detection. Genomics, Proteomics & Bioinformatics 2017, 15 (2), 59–72.
115. Huang Y; Zhu H, Protein Array-based Approaches for Biomarker Discovery in Cancer. Genomics, Proteomics & Bioinformatics 2017, 15 (2), 73–81.
116. Li Q; Zhou S; Zhang T; Zheng B; Tang H, Bioinspired sensor chip for detection of miRNA-21 based on photonic crystals assisted cyclic enzymatic amplification method. Biosensors and Bioelectronics 2020, 150, 111866. [PubMed: 31744650]
117. Blair S; Garcia M; Davis T; Zhu Z; Liang Z; Konopka C; Kauffman K; Colanceski R; Ferati I; Kondov B; Stojanoski S; Todorovska Magdalena B; Dimitrovska Natasha T; Jakupi N; Miladinova D; Petrusevska G; Kondov G; Dobrucki Wawrzyniec L; Nie S; Gruev V, Hexachromatic bioinspired camera for image-guided cancer surgery. Science Translational Medicine 2021, 13 (592), eaaw7067.
118. Sun W; Lee J; Zhang S; Benyshek C; Dokmeci MR; Khademhosseini A, Engineering Precision Medicine. Adv Sci (Weinh) 2018, 6 (1), 1801039–1801039. [PubMed: 30643715]
119. Wang Y; Springer S; Mulvey Carolyn L; Silliman N; Schaefer J; Sausen M; James N; Rettig Eleni M; Guo T; Pickering Curtis R; Bishop Justin A; Chung Christine H; Califano Joseph A; Eisele David W; Fakhry C; Gourin Christine G; Ha Patrick K; Kang H; Kiess A; Koch Wayne M; Myers Jeffrey N; Quon H; Richmon Jeremy D; Sidransky D; Tufano Ralph P; Westra William H; Bettegowda C; Diaz Luis A; Papadopoulos N; Kinzler Kenneth W; Vogelstein B; Agrawal N, Detection of somatic mutations and HPV in the saliva and plasma of patients with head and neck squamous cell carcinomas. Science Translational Medicine 2015, 7 (293), 293ra104–293ra104.
120. Jiang W-W; Rosenbaum E; Mambo E; Zahurak M; Masayesva B; Carvalho AL; Zhou S; Westra WH; Alberg AJ; Sidransky D; Koch W; Califano JA, Decreased Mitochondrial DNA Content in Posttreatment Salivary Rinses from Head and Neck Cancer Patients. Clinical Cancer Research 2006, 12 (5), 1564. [PubMed: 16533782]
121. Mishra S; Saadat D; Kwon O; Lee Y; Choi W-S; Kim J-H; Yeo W-H, Recent advances in salivary cancer diagnostics enabled by biosensors and bioelectronics. Biosensors and Bioelectronics 2016, 81, 181–197. [PubMed: 26946257]
122. List of Cleared or Approved Companion Diagnostic Devices (In Vitro and Imaging Tools) | FDA (https://www.fda.gov/medical-devices/in-vitro-diagnostics/list-cleared-or-approved-companion-diagnostic-devices-in-vitro-and-imaging-tools).
123. Therascreen PIK3CA RGQ PCR Kit. (https://www.qiagen.com/).
124. NovoTTF™-100L System. (https://www.novocure.com/)
125. Sangia Total PSA Test. (https://www.opko.com/).
126. BioIntelliSense BioSticker. (https://biointellisense.com/).
127. Optune. (https://www.optune.com/).
128. NovoTTF-200T. (https://www.novocure.com/).
129. PHESGO. (https://www.gene.com/patients/medicines/phesgo).
130. Gao W; Emaminejad S; Nyein HYY; Challa S; Chen K; Peck A; Fahad HM; Ota H; Shiraki H; Kiriya D; Lien D-H; Brooks GA; Davis RW; Javey A, Fully integrated wearable sensor arrays for multiplexed in situ perspiration analysis. Nature 2016, 529 (7587), 509–514. [PubMed: 26819044]

131. Abellán-Llobregat A; Jeerapan I; Bandodkar A; Vidal L; Canals A; Wang J; Morallón E, A stretchable and screen-printed electrochemical sensor for glucose determination in human perspiration. Biosensors and Bioelectronics 2017, 91, 885–891. [PubMed: 28167366]

132. Dexcom-continuous-glucose-monitoring What is Continuous Glucose Monitoring (CGM)? https://www.dexcom.com/continuous-glucose-monitoring.

133. Koh A; Kang D; Xue Y; Lee S; Pielak RM; Kim J; Hwang T; Min S; Banks A; Bastien P; Manco MC; Wang L; Ammann KR; Jang K-I; Won P; Han S; Ghaffari R; Paik U; Slepian MJ; Balooch G; Huang Y; Rogers JA, A soft, wearable microfluidic device for the capture, storage, and colorimetric sensing of sweat. Science translational medicine 2016, 8 (366), 366ra165–366ra165.

134. Bariya M; Shahpar Z; Park H; Sun J; Jung Y; Gao W; Nyein HYY; Liaw TS; Tai L-C; Ngo QP; Chao M; Zhao Y; Hettick M; Cho G; Javey A, Roll-to-Roll Gravure Printed Electrochemical Sensors for Wearable and Medical Devices. ACS Nano 2018, 12 (7), 6978–6987. [PubMed: 29924589]

135. Brolis-Sensor-Technology Blood analysis sensor. https://brolis-sensor.com/.

136. Bayoumy K; Gaber M; Elshafeey A; Mhaimeed O; Dineen EH; Marvel FA; Martin SS; Muse ED; Turakhia MP; Tarakji KG; Elshazly MB, Smart wearable devices in cardiovascular care: where we are and how to move forward. Nature Reviews Cardiology 2021, 18 (8), 581–599. [PubMed: 33664502]

137. Medical Devices Cleared or Approved by FDA in 2019. (https://www.fda.gov/medical-devices/recently-approved-devices/2019-device-approvals).

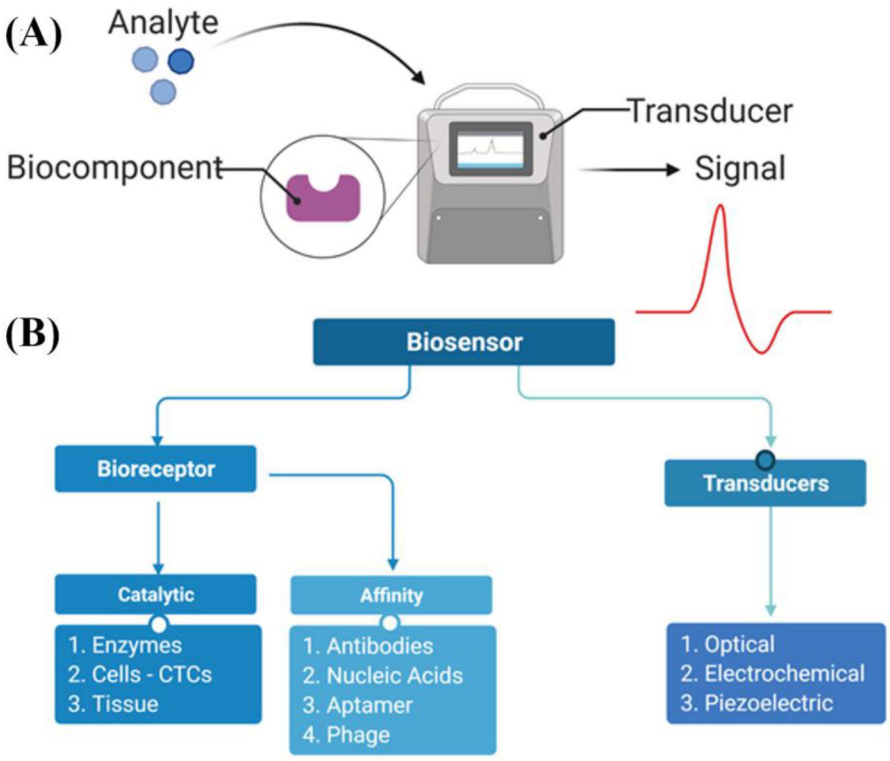

Figure 1.

Biosensor components **(A)** (Reproduced with permission from ref 5, copyright 2009 Elsevier); Classification of biosensors **(B)** (Reproduced with permission from ref 7, copyright 2020 MDPI)

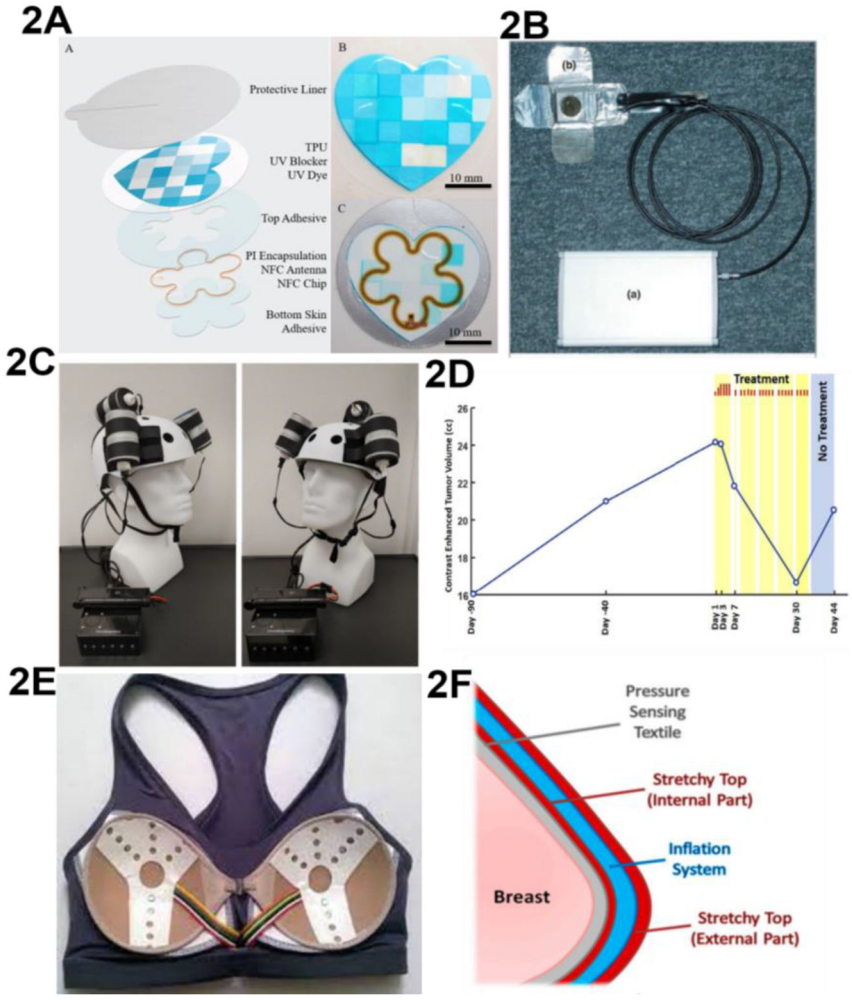

Figure 2.

Adhesive patch “My UV Patch”, to detect UV exposure **(2A)** (Reproduced with permission from ref 26, copyright 2018 Public Library of Science); OLED-based WDB device **(2B)** (Reproduced with permission from ref 28, copyright 2009 British Association of Dermatologists); Oncomagnetic WDB is a helmet with 3 oncoscillators secured on it **(2C)** and the graph displays the variation in contrast enhanced tumor (CET) volume over time **(2D)** (Reproduced with permission from ref 29, copyright 2021 Frontiers Media S.A.); High-tech iTBra is a smart WDB that can accurately detect breast cancer early **(2E)** (Reproduced with permission from ref 31, Copyright 2019 Elsevier); Palpreast system of the top view of the internal layer, and inflation process **(2F)** (Reproduced with permission from ref 32, copyright 2019 MDPI)

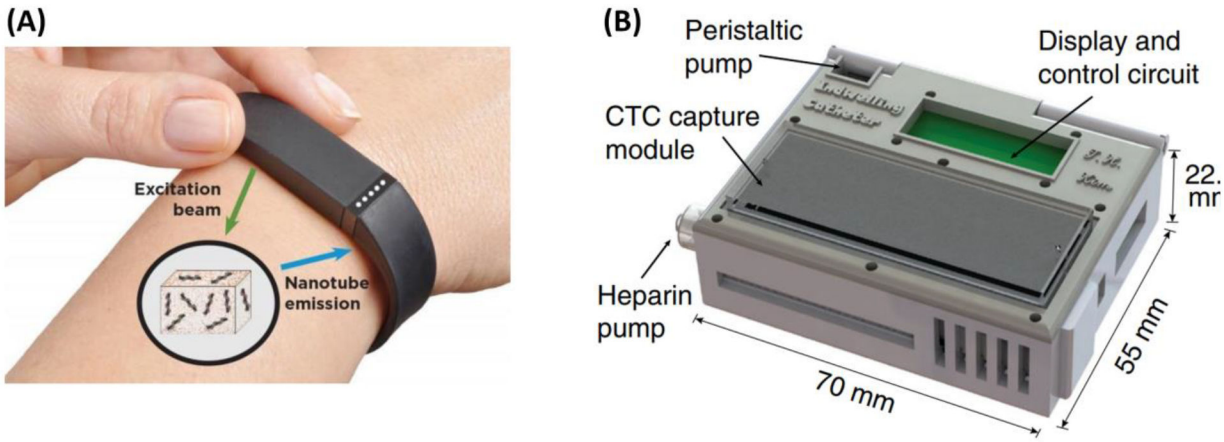

Figure 3.

Optical cancer detector is a small WDB worn on the wrist and send the excitation beams into the sensors where the light is analyzed and emitted via nanotube emission to furnish continuous updates **(A)** (Reproduced with permission from ref 34, Copyright 2017 American Society of Mechanical Engineers); The *in vivo* aphaeretic CTC isolation system **(B)** (Reproduced with permission from ref 35, Copyright 2019 Springer Nature)

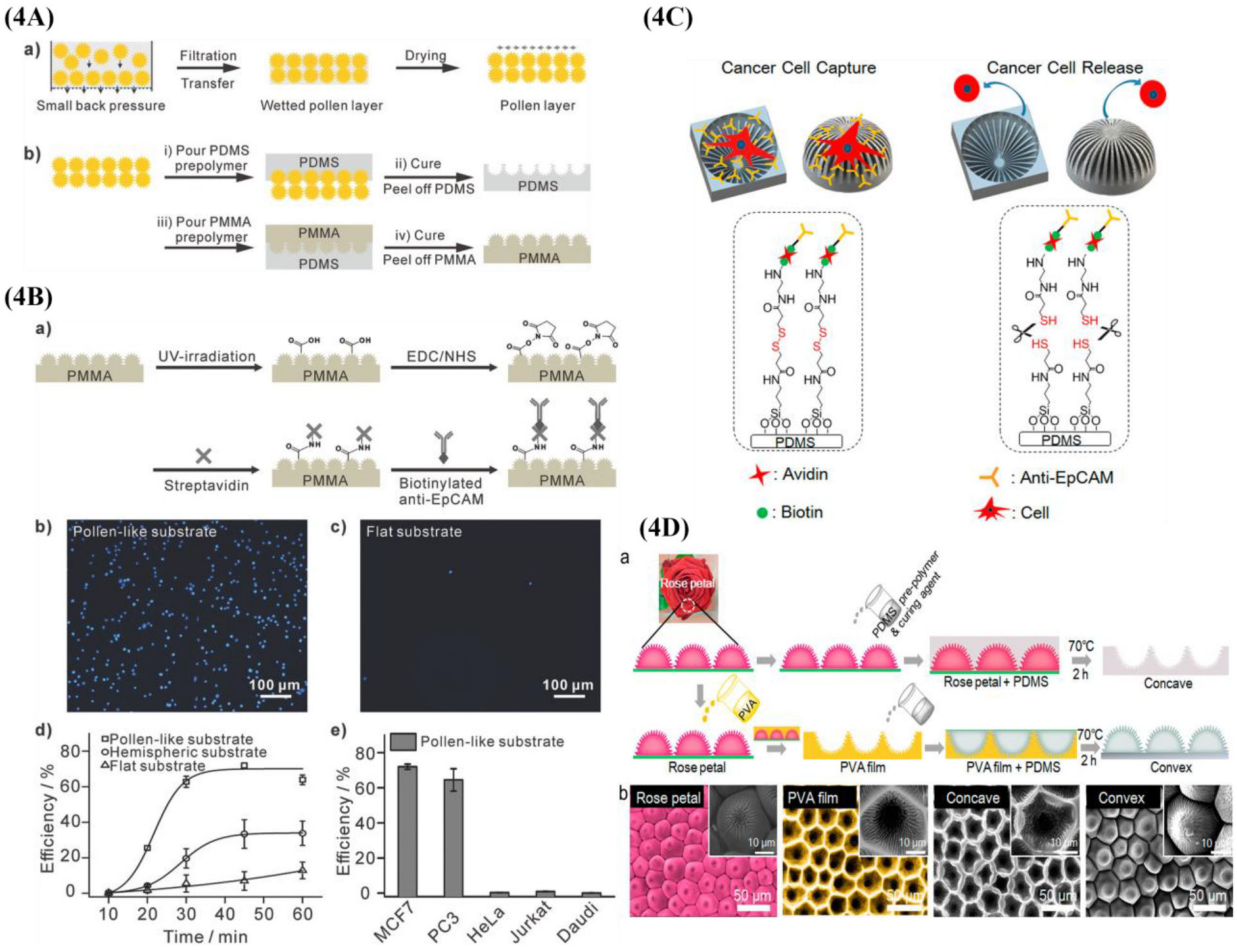

Figure 4.

Schematic diagram for synthesis of the pollen-like substrates with two steps process (**4A**), and cell capture efficiency with functionalization by anti-EpCAM biomarker (**4B**) (Reproduced with permission from ref 50, Copyright 2017 John Wiley and Sons); Schematic diagram of anti-EpCAM conjugated substrate for CTC capture and release (**4C**), Fabrication process and SEM images of the CTC-capturing structure (**4D**) (Reproduced with permission from ref 51, Copyright 2017, American Chemical Society)

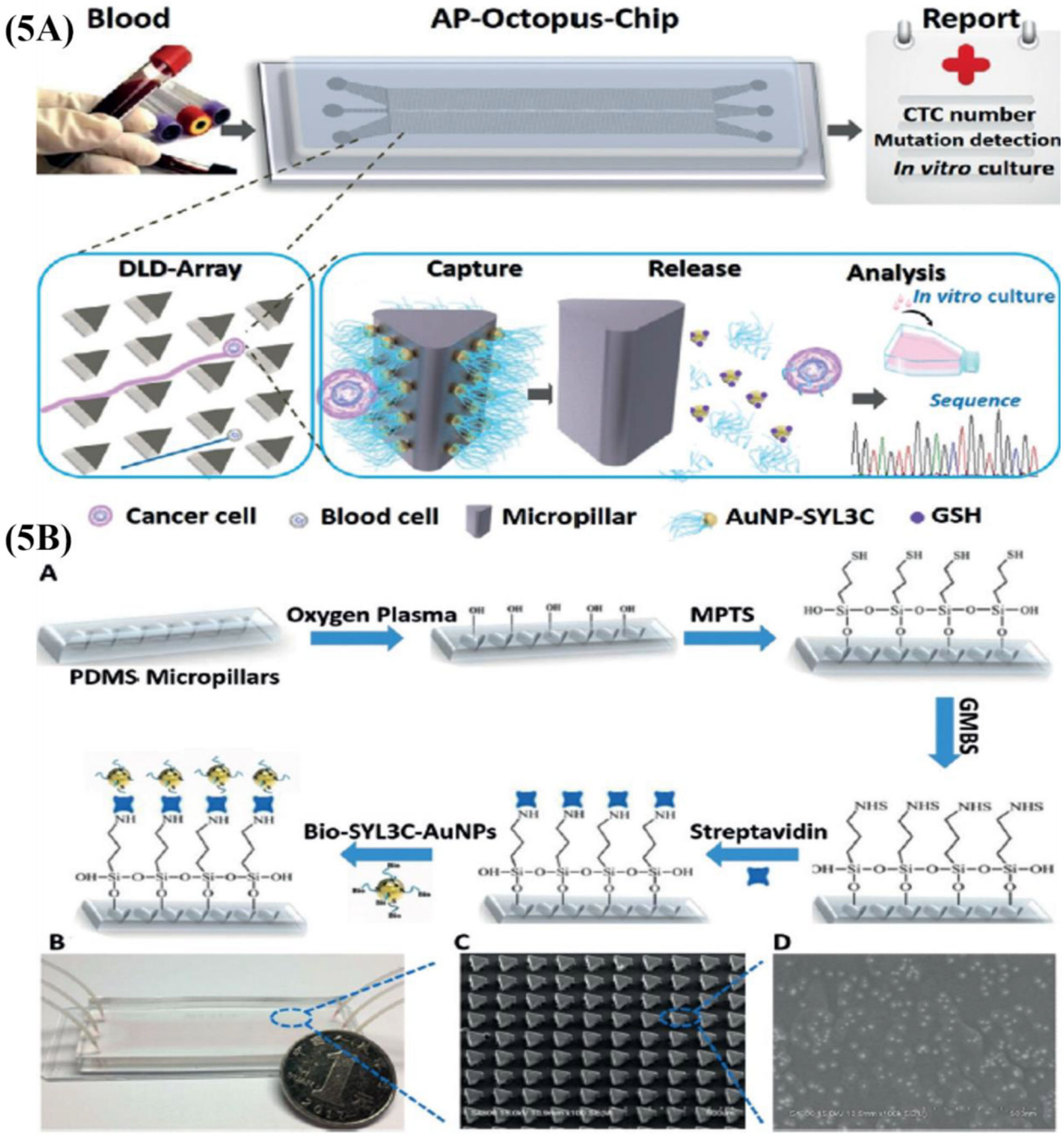

Figure 5.

Schematic diagram of the AP-Octopus-Chip: (**5A**) Mechanism of capturing and releasing cancer cells, (**5B**) Schematic diagram of chemical modification and surface adhesion process of the AP-Octopus Chip along with SEM images of the microarray arrangement (Reproduced with permission from ref 52, Copyright 2019 Wiley-VCH Verlag GmbH & Co. KGaA, Weinheim)

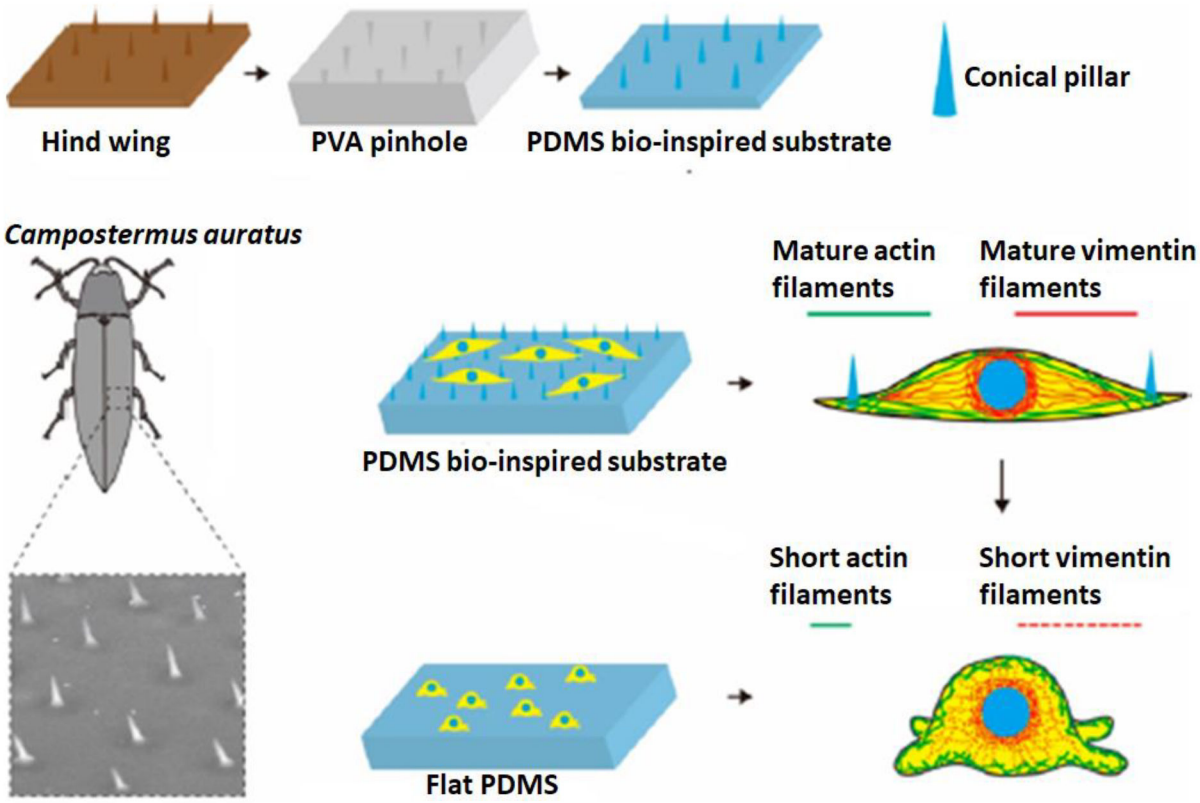

Figure 6.

Schematic diagram of cell attachment on canonical pillar-based PDMS substrate and flat PDMS substrate showing the arrangement of actin and vimentin filaments within cell cytoplasm (Reproduced with permission from ref 53, Copyright 2018 American Chemical Society)

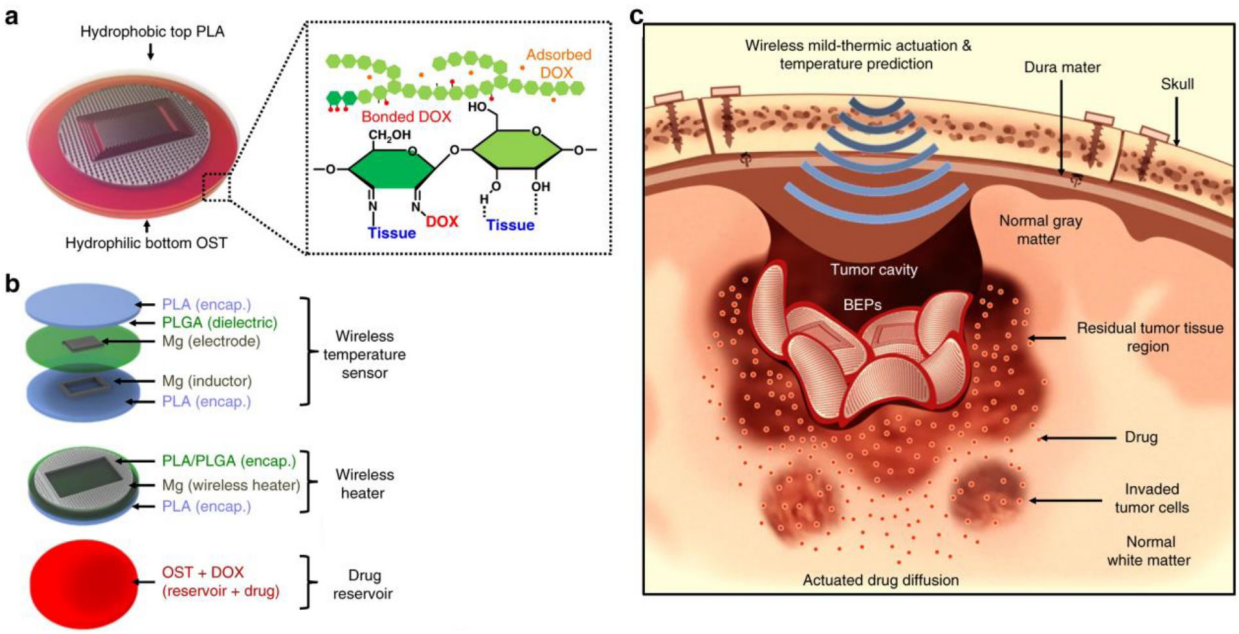

Figure 7.

Schematic diagram and prototype of bioresorbable electronic patch (BEP) with layered structure of hydrophobic and hydrophilic assembly. The system was loaded with doxorubicin for cancer cell inhibition (Reproduced with permission from ref 69, Copyright 2019 Springer Nature).

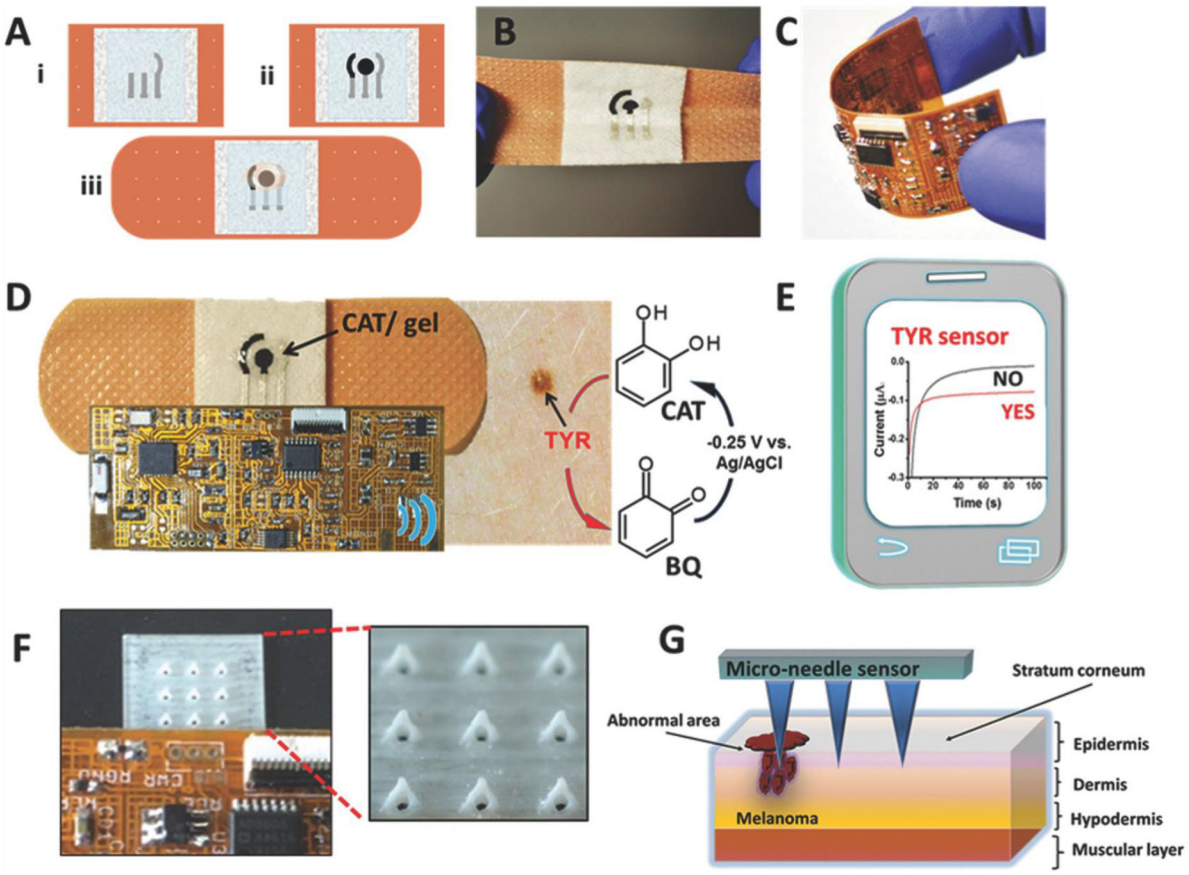

Figure 8.

Schematic diagram and prototype of bandage based flexible sensor with carbon and Ag/AgCl (insulator) ink printed microneedle device to evaluate catechol (CAT) oxidation by forming benzoquinone (BQ) in the presence tyrosinase (TYR) (Reproduced with permission from ref 82, Copyright 2018 WILEY-VCH Verlag GmbH & Co. KGaA, Weinheim)

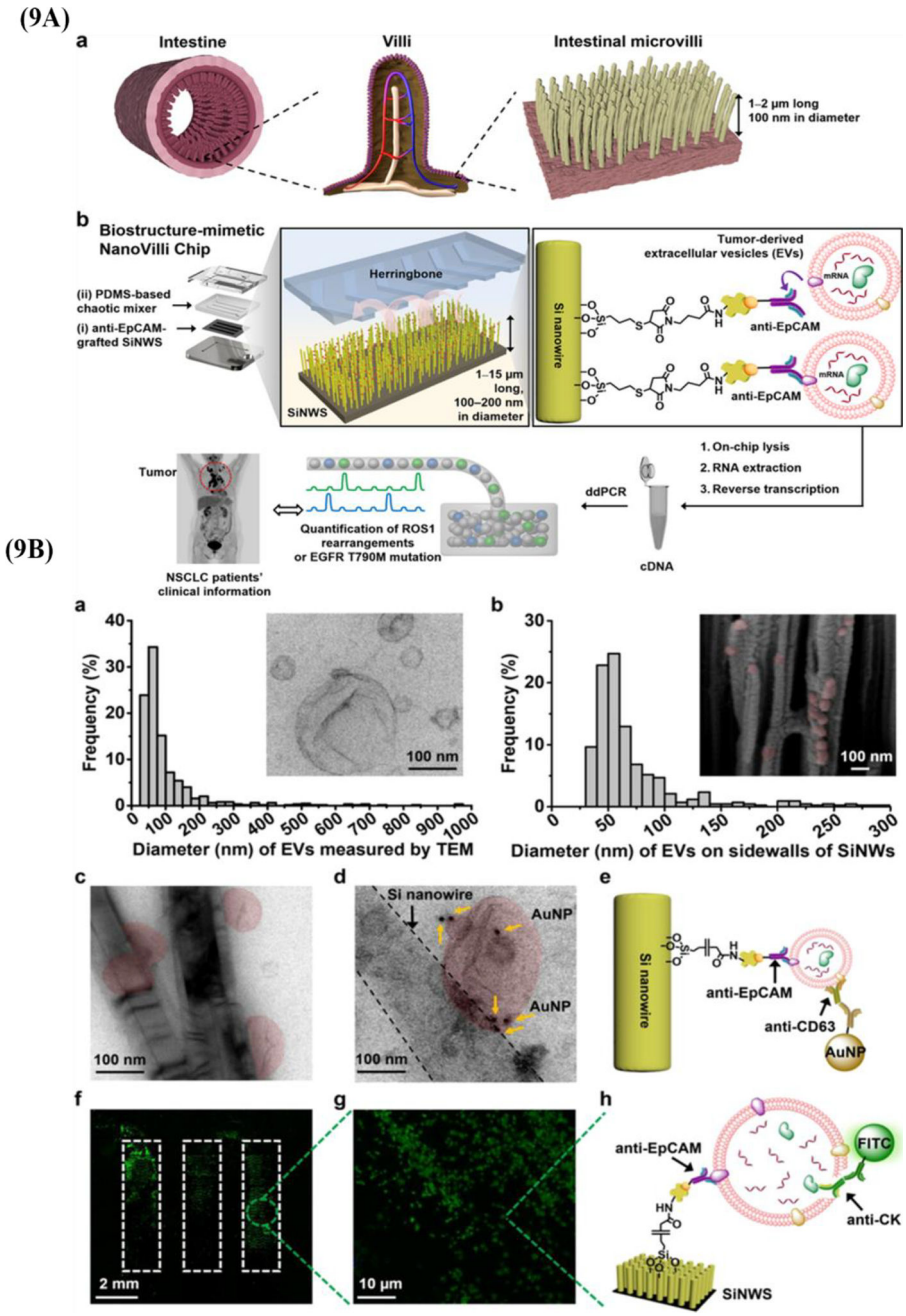

Figure 9.

Schematic diagram of biomimetic fabrication of NanoVilli chip based on the inspiration of intestinal microvilli, Si nanowire functionalization with anti-EpCAM biomarker **(9A)** and characterization of captured EVs **(9B)** (Reproduced with permission from ref 83, Copyright 2019 American Chemical Society)

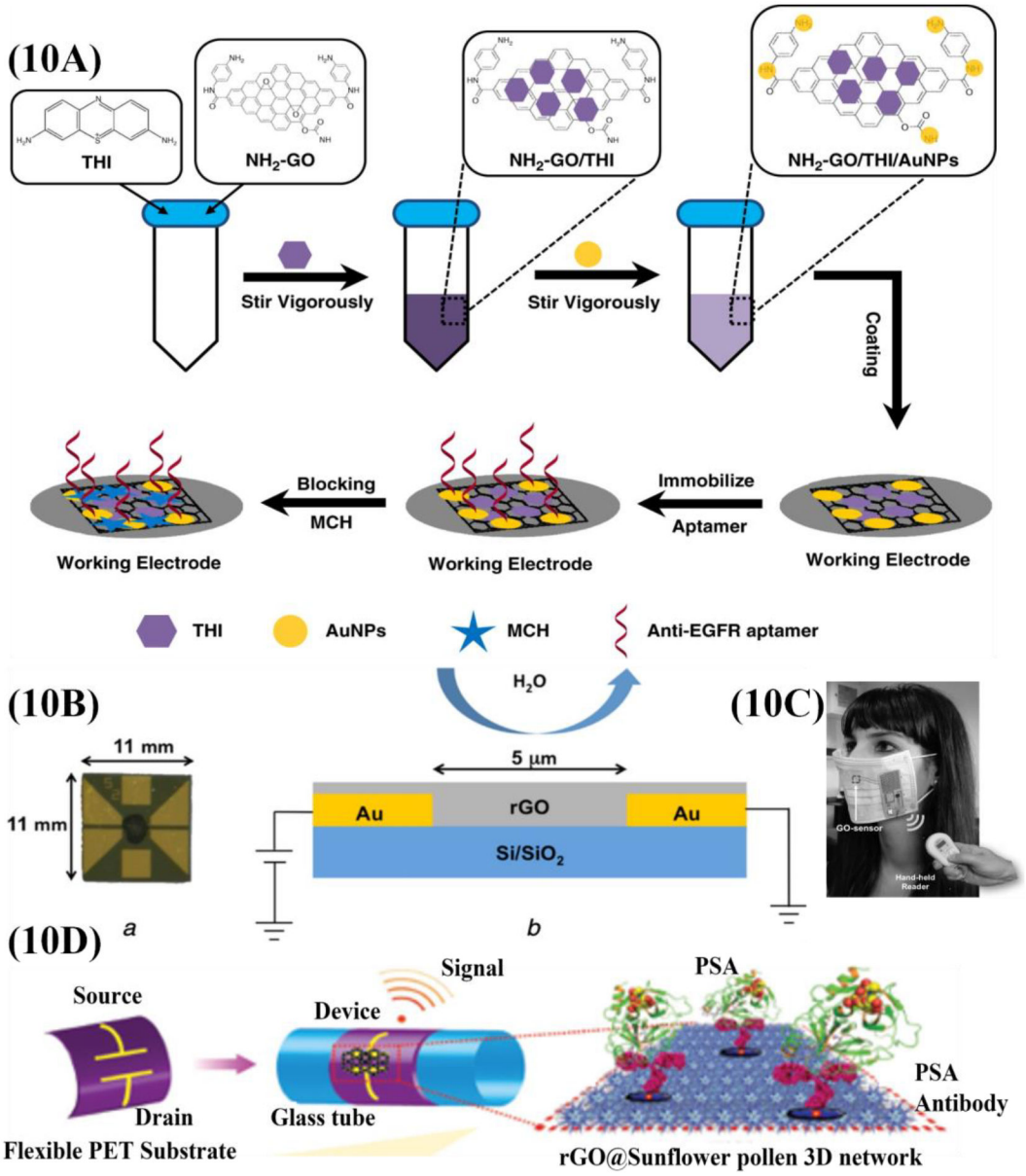

Figure 10.

Schematic diagram of fabrication process of functionalized origami-paper with anti-EGFR aptamer **(10A)** (Reproduced with permission from ref 95, Copyright 2020 Springer Nature); rGO based prototype for lung cancer detection **(10B)** and integrated wireless readout for detection **(10C)** (Reproduced with permission from ref 97, Copyright 2018 The Institution of Engineering and Technology); Schematic diagram of rGO-sunflower pollen (SFP) coated flexible PET for prostate cancer detection **(10D)** (Reproduced with permission from ref 98, Copyright 2016 WILEY-VCH Verlag GmbH & Co. KGaA, Weinheim)

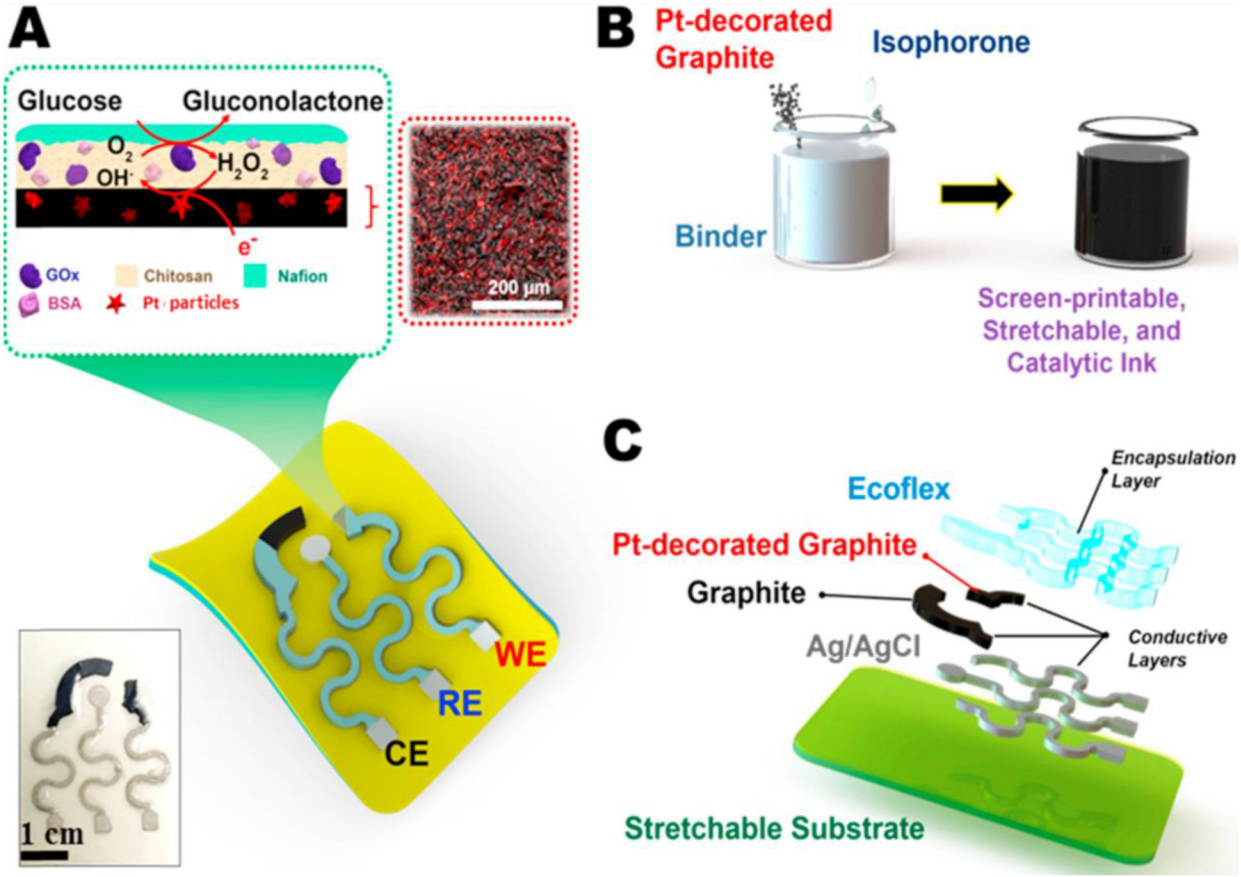

Figure 11.

Schematic representation of the stretchable sensor, enzymatic immobilization on the printed catalytic layer, and the interactions during detection. The inset shows actual photograph of a screen-printed sensor (Reproduced with permission from ref 131, Copyright 2017 Elsevier B.V. All rights reserved).

Table 1:

Summary of Lab-on-a-chip (LOC) devices for detection and diagnosis of cancer disease

Research group	Lab-on-a-chip (LOC) design	Analyte of Interest	Ref
Yildiz et al.	MiSens LOC device integrated with microfluidic systems.	PSA	19
Parra-Cabrera et al.	LOC device consisted of gold electrodes designed in a series array in a fluidic microchannel.	PSA and spondin-2 (SPON2).	20
Jiwei et al.	Metabolic enzymes decorated LOC sensor	PSA and AMACR	21
Akbari et al.	Sandwich typed electrode of GO/AuNPs	PSA	22
Indra et al.	Non-faradaic biosensor, a lectin-assisted capacitive sensor	PSMA	23
Juliana et al.	Single-stranded DNA probe with LbL pattern of chitosan and MWCNT	PCA3	24

Table 2:

WDBs and respective core technologies for detection and diagnosis of cancer.

Manufacturer	Device/Type	Application area	Ref
La Roche-Posay	UV patch	Measure skin exposure to UV radiation and early diagnosis of skin cancer.	25–27
Attili et. al.	Photodynamic therapy	Efficient therapy for non-melanoma skin cancer.	28
Baskin et al.	Oncomagnetic WDB	Reduced contrast-enhanced tumor (CET) volume	29
Bahrami et al.	Ultra-wideband	Cancer diagnosis	30
Cyrcadia Health and Nanyang Technological University, Singapore	iTBra	Detects early breast cancer symptom by sensing the breast tissues for any circadian temperature changes	31
Arcarisi et al.	Palpreast	Self-examination of breast and for early diagnosis of breast cancer	32
Teng et al.	WDB probe	Monitoring in breast cancer neoadjuvant chemotherapy infusions	33
Memorial Sloan Kettering Cancer Center, USA	Wrist band	Identify cancer type and stage	34
Hayes et al.	Intravascular aphaeretic WDB	CTC isolation and capturing from peripheral vein	35

Table 3:

Materials diversity for fabrication of WDBs and LOC sensors for cancer detection.

Material type	Research group	Selected materials for the synthesis	Feature/Characteristics	Ref
Synthetic materials	Wang et al.	PMMA along with UV curing agent assisted pollen layered structure PDMS decorated with anti-EpCAM	Cancer cell isolation	50
	Dou et al.	PDMS coated on rose petals, and loaded with anti-EpCAM	CTCs isolation	51
	Song et al.	DLD arrangement on PDMS with Au and anti-EpCAM aptamer	Elevated capture efficiency and prevented the possible damage of the captured cancer cells	52
	Su et al.	Paclitaxel (PTX) loaded poly (caprolactone)-ester end-capped nanoparticle coated with RBC and decorated with NIR responsive dye	Prolonged circulation, drug release along with PTT effect on cancer cells	55
	Han et al.	Amphiphilic diblock copolymer loaded with NIR responsive dye	NIR imaging and PTT on cancer cells	56
	Rahman et al.	Flexible substrate of 5-(4-(perfluorohexyl) phenyl)thiophene-2-carbaldehyde as an antenna substrate	Early detection of breast cancer	57
Biobased materials	Bharathi et al.	chitosan/copper oxide CS-CuO) using a plant extracted bioflavonoid, Rutin	Anti-proliferation effect against human lung cancer cells with increased apoptosis.	58
	El Assal et al.	cryoprotectants with dextran and carboxylated ε-poly-L-lysine (CPLL)	human cytokine activated natural killer (NK) cell conservation without altering cytotoxic strength for cancer immunotherapy.	62
	Zhong et al.	cellulose nano-micelle derived from (MCC-graft-PPDO) copolymer	Cancer cells imaging as early detection modalities	63
	Mansur et al.	Fluorescent alloyed-ZnCdS quantum dot-based core and carboxymethylcellulose (CMC) based shells	Cancer cell bio-labeling for oncology applications.	64
	Garg et al.	Heparin modified-cellulose acetate phthalate (HEC) nanoparticles	Cytotoxic effects of usnic acid (UA) following treatment to lung cancer cells	65
	Hazra et al.	Hydroxyl group of cellulose functionalized with iron oxide nanoparticle and Transferrin	Isolating and capturing circulating tumor cells (CTCs) from head and neck cancer patient's blood sample	66
	Maier et al.	Persian Blue loaded cellulose paper-based sensor integrated with two printed carbon-based electrodes	Early detection of lung cancer with high detection ability of this sensor towards hydrogen peroxide (H_2O_2)	68
	Lee et al.	PLA and PLGA based multilayered electronic patch with magnesium-based sensors in the core	Hydrophobic and hydrophilic arrangement enabled the device to stick on the localized tumor provide sustain drug release to suppress the tumor volume and elevated survival rate in vivo	69
Metal nanoparticles and complexes	An et al.	Benzoboric acid functionalized gold-plated PDMS substrate in 3D regular pattern arrangement	Larger surface area of the pattern arrangement provided crucial role for CTC capturing	70
	Chen et al.	$FeCl_3$ conjugated (PMPC-b-PserA) polymer and loaded with curcumin	release curcumin and inhibit breast cancer cells	72
	You et al.	Gold nanoshells coated with BSA functionalized Gd and loaded with ICG	photothermal effect and synergistic effect of photodynamic therapy on localized tumor cells	73

Material type	Research group	Selected materials for the synthesis	Feature/Characteristics	Ref
	Chen et al.	bacteria-like spiky MOFs of aluminium (Al) sulfate with ruthenium (III) (Ru) chloride hydrate	Photothermal effect on local tumor region causing stress on tumor cells (promoting antitumor immunity) and Al salt recruited immune cells	74
	Huang et al.	DOX loaded poly (lysine) attached with DTSSP and amino group-modified superparamagnetic iron oxide nanoparticles (SPIO-NH_2) along with Indocyanine (ICG)-coated with cancer cell membrane (CCM)	Coating with CCM promoted nanoparticles to adhere to tumor cells and photothermal effect promoted the release of DOX. Presence of SPIO and ICG helped to monitor the system.	77
	Zhang et al.	HeLa cancer cell membrane disguised in zeolitic imidazolate framework 8 (ZIF-8) based MOF nanoparticles	Suppress PLK1 gene for lung cancer growth.	78
	Mukherjee et al.	Biosynthesized gold nanoparticles tagged with DOX	Effective inhibition towards proliferation and growth of cancer cells	79
	Kim et al.	$CuInS_2$/ZnS quantum dots system	Tumor imaging system	80
	Hou et al.	Transferrin conjugated hollow mesoporous CuS nanoparticles loaded with iron dependent artesunate (AS)	localized drug delivery, optical imaging, photoacoustic tomography and immunofluorescence followed by peritumoral (PT) injection with NIR irradiation for cancer diagnosis	81
	Ciui et al.	Ag/AgCl ink and PS-PI-PS based Ercon carbon ink layers followed by coating of an insulating layer	Flexible bandage-based sensors for detection of skin melanoma	82
0 – 3D nanostructure	Dong et al.	Silicon nanowire arrays in an arrangement on PDMS substrate and functionalization with Anti-EpCAM biomarker	Promote enhanced efficiency for capturing tumor derived extracellular vesicles (EVs) from blood plasma	83
	Haslam et al.	Graphene field effect transistor immunosensors synthesized using CVD technique on Si/SiO_2 substrate by photolithography and functionalized with anti-hCG antibody	Detection of Human Chorionic Gonadotropin (hCG) glycoprotein for cancer cells	84
	He et al.	RBC membrane that disguised 2D $MoSe_2$ nanosheets synthesized via liquid exfoliation techniques.	PTT on tumor cells by stopping macrophage phagocytosis and enhancing hemocompatibility and circulation time	85
	Zhang et al.	DOX loaded Magneto-fluorescent system with iron carbon quantum dots conjugated with a folic acid and riboflavin	Targeted drug release using imaging and PDT/PTT synergistic effects on cancer cells via application of NIR irradiation	86
	Zhang et al.	Coating on SWCNTs with Fe_3O_4 conjugated carbon quantum dots through PEG linker and loaded with DOX	Targeted drug release and imaging for PDT and PTT applications against cancer cells	87
	Wu et al.	SWNT functionalized with RGD peptide and replicated from ATMV virus subunit arrays	Penetrate to neighboring infected cells and reach deep in tumor cells to start lysis.	88
	Marangon et al.	MWCNT arranged in π–π stacking and loaded with photosensitizer	PTT, PDT, and an integrated therapy on cancer cells	89
	Xie et al.	SWCNT system with Evans Blue as dispersion agent for long circulation and loaded with albumin conjugated fluorescent photosensitizer, Chlorin e6 (Ce6)	Fluorescent and photoacoustic imaging of tumors along with synergistic use with PDT and PTT for effective tumor ablation effect.	91
	Yin et al	MnO_2 flakes coated and crosslinked on CNTs and loaded with Chlorin e6 (Ce6)	PDT, PTT and fluorescence imaging on cancer cells	92
	Cao et al.	PEGylated nano-graphene oxide loaded with Chlorin e6	PDT, PTT, or integrated therapy, diffusion-weighted and blood oxygenation level dependent MRI	93
	Shim et al.	Clostridium perfringens enterotoxin (CPE) loaded with chlorin e6 (Ce6) separated by PEG spacers and conjugated on the surface of rGO	PTT on cancer cells	94

Material type	Research group	Selected materials for the synthesis	Feature/Characteristics	Ref
	Wang et al.	EGFR with functionalization of amine groups of graphene with thionine (THI) and gold nanoparticles (AuNPs) and decorated with anti-EGFR	Capture cancer cells with elevated detection signal for higher accuracy.	95
	Caccami et al.	RFID sensors with substrate of Si/SiO_2 with p-type doped silicon wafer and coated with rGO decorated with biomarker	Early detection of cancer	97
	Wang et al.	rGO-sunflower pollen particles and coated on PET substrate patterned with Au/Pt electrodes and decorated with anti-PSA antibodies	Identify the prostate cancer cells	98
Protein based systems	Damiati et al	Folate modified bacterial surface layer protein (SbpA) on gold substrate	Sensor for breast cancer detection with higher efficiency and differentiate between MCF-7 and HepG2 cancer cells	99
	Tan et al.	bioinspired lipoprotein (bLP) loaded with photothermal agent and mertansine (M-bLP) anticancer drug	Drug release and PTT effect on cancer cells	100
	Han et al.	Conjugated GEM to HAS with cleavable peptide GFLG and tagged with NIR dye	Enzyme responsive albumin-based gemcitabine (GEM) loaded delivery system for chemotherapy and PTT	101
	Sim et al.	HSA nanoparticles loaded with melanin and paclitaxel (PTX)	Efficient tumor chemotherapy for long circulation	102
	Li et al.	HSA-based nanoparticles functionalized with Pt(IV) antitumor prodrug, NIR fluorophore, Cy5, and quencher Qsy21	Tumor cell imaging along with localized triggering of Pt(IV) prodrug and providing a theranostic effect	103
	Hu et al.	Thermo-responsive reactive oxygen species (ROS) by functionalization of HSA-chlorin e6 nano-assemblies	PDT against cancer cells	104
	Chen et al.	Conjugated HSA with hemoglobin and loaded with photosensitize chlorin e6	PDT on cancer cells	105
	Wang et al.	ultra-small copper sulfide (CuS) nanoparticles within the ferritin (Fn) nanocages	PTT for cancer theranostics, photoacoustic imaging (PAI) and PET imaging	106
	Khandare et al.	Transferrin, Anti-EpCAM, pan-cytokeratins (CKs) 8, 18, 19 antibody conjugated systems	Isolate and capture CTCs from head and neck cancer patient's blood sample	107

Table 4:

FDA approved WDB devices, sensor and detection kit used for cancer treatment

Research group	Devices	Application area	Ref
Qiagen™	The Therascreen PIK3CA RGQ PCR Kit - P190001 and P190004	Breast cancer	123
Novocure™	NovoTTF™-100L System - H180002	Malignant Pleural Mesothelioma	124
OPKO Diagnostics, LLC	Sangia Total PSA Test -P170037	Diagnosis of prostate cancer	125
BioSticker™	BioIntelliSense BioSticker	Data services for clinical trials of hematological cancer patients	126
Optune®	Optune	Diagnosis of glioblastoma (GBM)	127
Novocure™	NovoTTF-200T	Advanced Liver Cancer	128
Genentech	PHESGO™, pertuzumab, trastuzumab and hyaluronidase	Breast cancer	129

Table 5:

FDA approved WDB devices, sensor and detection kit used for diagnosis beside cancer treatment[137] (Table reproduced from [137])

Device name	Application area
CentriMag Circulatory Support System - P170038	Blood Pump
FoundationOne®CDx - P170019/S006	Laboratory Test
LIAISON QuantiFERON-TB Gold Plus, LIAISON Control QuantiFERON-TB Gold Plus, LIAISON QuantiFERON Software - P180047	Laboratory Test
Tula® System - P190016	Ear Tubes
IN.PACT AV Paclitaxel-coated Percutaneous Transluminal Angioplasty (PTA) Balloon Catheter - P190008	Balloon Catheter
MiSight 1 Day (omafilcon A) Soft (Hydrophilic) Contact Lenses for Daily Wear – P180035	Contact Lenses
Axonics Sacral Neuromodulation (SNM) System for Urinary Control – P180046	Urinary Retention
Myriad myChoice CDx - P190014	Laboratory Test
LIAISON XL MUREX HCV Ab, LIAISON XL MUREX Control HCV Ab - P190011	Laboratory Test
iDESIGN® Refractive Studio and STAR S4 IR® Excimer Laser Systems – P930016/S057	Laser Vision Correction
Axonics Sacral Neuromodulation (SNM) System - P190006	Incontinence
Alcon Laboratories, Inc. AcrySof® IQ PanOptix® Trifocal Intraocular Lens (Model TFNT00) and AcrySof® IQ PanOptix® Toric Trifocal Intraocular Lens (Models TFNT30, TFNT40, TFNT50, TFNT60) - P040020/S087	Intraocular Lens
Minimally Invasive Deformity Correction (MID-C) System - H170001	Spine
BAROSTIM NEO System - P180050	Heart Failure
The Tether™ - Vertebral Body Tethering System - H190005	Spine
Medtronic CoreValve Evolut R System and Medtronic CoreValve Evolut PRO System - P130021/S058	Heart Valve
Edwards SAPIEN 3 Transcatheter Heart Valve System and Edwards SAPIEN 3 Ultra Transcatheter Heart Valve System - P140031/S085	Heart Valve
PD-L1 IHC 22C3 pharmDx - P150013/S016	Laboratory Test
MED-EL Cochlear Implant System - P000025/S104	Cochlear Implant
Medtronic CoreValve System; Medtronic CoreValve Evolut R System; Medtronic CoreValve Evolut PRO System - P130021/S033	Heart Valve
PD-L1 IHC 22C3 pharmDx - P150013/S014	Laboratory Test
HeartStart OnSite Defibrillator (Model M5066A), HeartStart Home Defibrillator (Model M5068A), Primary Battery (Model M5070A), SMART Pads Cartridges (Adult Model M5071A) and Infant/Child (Model M5072A) - P160029	Defibrillator
Eversense Continuous Glucose Monitoring System - P160048/S006	Glucose Monitor
Hintermann Series H3™ Total Ankle Replacement System - P160036	Joint Replacement
TransMedics OCS Lung System - P160013/S002	Lung Donor
Neuroform Atlas® Stent System - P180031	Stent
VICI VENOUS STENT® System - P180013	Stent
Tack Endovascular System® (6F) - P180034	Vascular
XVIVO Perfusion System (XPS™) with STEEN Solution™ Perfusate - P180014	Perfusion System
LOTUS Edge™ Valve System - P180029	Heart Valve
TransPyloric Shuttle/TransPyloric Shuttle Delivery Device - P180024	Weight Loss
TherOx DownStream System - P170027	Oxygen Therapy
Cerene Cryotherapy Device - P180032	Menstrual Bleeding
TRILURON™ - P180040	Osteoarthritis
OPTIMIZER Smart System - P180036	Cardiovascular

Device name	Application area
MitraClip NT Clip Delivery System and MitraClip NTR/XTR Clip Delivery System - P100009/S028	Vascular
VENOVO Venous Stent System - P180037	Stent
COVERA™ Vascular Covered Stent - P170042/S002	Stent
VENTANA PD-L1 (SP142) Assay - P160002/S009	Hernia
M6-C™ Artificial Cervical Disc - P170036	Spine
MANTA Vascular Closure Device - P180025	Vascular